

RESEARCH ARTICLE

Importance of regional indices of atmospheric circulation for periods of warming and cooling in Svalbard during 1920–2018

Ewa B. Łupikasza¹  | Tadeusz Niedźwiedź¹ | Rajmund Przybylak^{2,3}  | Øyvind Nordli⁴

¹University of Silesia in Katowice, Faculty of Natural Sciences, Institute of Earth Sciences, Sosnowiec, Poland

²Department of Meteorology and Climatology, Nicolaus Copernicus University, Faculty of Earth Sciences and Spatial Management, Toruń, Poland

³Centre for Climate Change Research, Nicolaus Copernicus University, Toruń, Poland

⁴Department of Research and Development, Division for Model and Climate Analysis, Norwegian Meteorological Institute, Oslo, Norway

Correspondence

Ewa B. Łupikasza, University of Silesia in Katowice, Faculty of Natural Sciences, Institute of Earth Sciences, Sosnowiec, Poland.

Email: ewa.lupikasza@us.edu.pl

Funding information

National Science Centre, Poland, Grant/Award Number: 2015/19/B/ST10/02933

Abstract

The Arctic has experienced prominent climate warming, at the beginning of the 20th century and currently. Comparing the driving mechanism during these periods helps to explain the causes of contemporary climate change. Our study explores the impact of regional circulation on Svalbard's surface air temperature (SAT, 2 m above ground). We used air temperature data from Svalbard Airport, Bjørnøya stations, and three regional circulation indices that describe the frequency of cyclonic conditions, zonal circulation, and meridional circulation. The indices were calculated for four circulation areas with differing circulation conditions and, therefore, may have various impacts on long-term changes in SAT. This was checked for the entire study period (1920–2018), and 30-year sub-periods representing the most prominent climatic events: the early 20th-century Arctic warming (ETCAW), contemporary Arctic warming (CAW), and a cold period between them (CAP). In autumn and winter, the deviations in SAT from the long-term average during warm and cold periods were almost twice as large at Svalbard Airport as at Bjørnøya. In these seasons, the ETCAW was significantly warmer than the subsequent cold period, which was not the case for summer and spring. However, long-term trends in the regional circulation indices were more evident in summer and spring than in autumn and winter. Air temperature was the most strongly influenced by meridional circulation over the eastern circulation areas, with the exception of spring, when air temperature variability was more affected by zonal circulation. The recent warming weakened the relationship between SAT and the indices in summer. We attributed the ETCAW in autumn to a southerly advection of sensible heat. During the same historical period, the impact of the indices was much weaker in winter. In winter during the CAP, there was a higher frequency of northern air advection, particularly over the northern part of the Greenland Sea.

KEYWORDS

air temperature, atmospheric circulation, climate change, contemporary warming, ETCW, Svalbard

1 | INTRODUCTION

Before the contemporary global warming, the early 20th-century warming was the second-most prominent climate phenomenon of a regional and seasonal scale (Johannessen *et al.*, 2004; Overland *et al.*, 2004; Serreze and Francis, 2006; Semenov, 2007; Wood and Overland, 2010; Turner and Marshall, 2011) that manifested in the Arctic and peaked at various times between 1920 and 1950 depending on the region and the season (Kelly *et al.*, 1982; Przybylak, 2000; Yamanouchi, 2011; Łupikasza and Niedźwiedź, 2019). The Early Twentieth Century Arctic Warming (hereinafter ETCAW) was intensely studied in the first half of the 20th century (Knipovich, 1921; Scherhag, 1931, 1937, 1939; Hesselberg and Birkeland, 1940; Vize, 1940; Weickmann, 1942; Groissmayer, 1943; Lysgaard, 1949) and has become a subject of in-depth studies again since the start of the contemporary warming and developing climate modelling (Delworth and Knutson, 2000; Przybylak, 2000; Serreze *et al.*, 2000; Bengtsson *et al.*, 2004; Johannessen *et al.*, 2004; Shiogama *et al.*, 2006; Wood and Overland, 2010; Yamanouchi, 2011; Semenov and Latif, 2012; Suo *et al.*, 2013; Brönnimann, 2015; Hegerl *et al.*, 2018; Wegmann *et al.*, 2018; Łupikasza and Niedźwiedź, 2019; Przybylak *et al.*, 2021). Considered mostly naturally driven (Bengtsson *et al.*, 2004; Johannessen *et al.*, 2004; Nozawa *et al.*, 2005; Johannessen *et al.*, 2016; Wegmann *et al.*, 2017, 2018), the ETCAW plays a crucial role in climate change research and is helpful in understanding the causes of the contemporary warming. Moreover, the event occurred when the rate of inter-decadal change in radiative forcing was much weaker (Tokinaga *et al.*, 2017).

Many factors have been considered to have contributed to the ETCAW, such as intensified solar radiation, and lull in volcanic activity (Robock, 2000), reduced sea-ice cover (Bengtsson *et al.*, 2004; Semenov and Latif, 2012; Brennan *et al.*, 2020) that modified sea surface temperature (Polyakov *et al.*, 2010) and enhanced turbulent heat fluxes from the ice-free sea (Wegmann *et al.*, 2018), Atlantic Multi-decadal Oscillation (Miles *et al.*, 2014; Johannessen *et al.*, 2016; Tokinaga *et al.*, 2017), and other feedback mechanisms that involve clouds and water vapour (Brönnimann, 2015). Grant *et al.* (2009) found that in the European Arctic during the first decade of the 20th century cold and unpolluted air from the Arctic basin was dominant, while in the 1930s, warm and sometimes heavily-polluted air masses from western Europe were prevalent. Based on these findings, he concluded that aerosols might have amplified the ETCAW by changing the cloud long-wave emissivity due

to various properties of air masses compared to the cold period of the 1910s. Despite all these factors, atmospheric circulation is suggested to play an early role on air temperature (Scherhag, 1931; Weickmann, 1942; Petterssen, 1949; Lamb and Johnsson, 1959); this has also been confirmed in later studies (Hanssen-Bauer and Førland, 1998; Przybylak, 2000, 2002, 2016; Bengtsson *et al.*, 2004; Nozawa *et al.*, 2005; Shiogama *et al.*, 2006; Grant *et al.*, 2009; Yamanouchi, 2011; Suo *et al.*, 2013; Tokinaga *et al.*, 2017; Wegmann *et al.*, 2017).

The contribution of atmospheric circulation to the ETCAW was assessed by both the modelling of climate processes and by studies based on station data which, however, are scarce for that period. A preference for more meridional circulation patterns was found over the high latitudes of the North Atlantic during the early 20th-century climatic fluctuation (Petterssen, 1949; Overland *et al.*, 2008; Grant *et al.*, 2009; Wood and Overland, 2010; Johannessen *et al.*, 2016; Svyashchennikov *et al.*, 2020). An increase in the intensity of southerly (Wood and Overland, 2010; Łupikasza and Niedźwiedź, 2019) or south-westerly to westerly flow (Bengtsson *et al.*, 2004) through the passage between Spitsbergen and Northern Norway into the Barents Sea contributed to ETCAW. Based on regional circulation types, air advection from the southern sector was assessed to explain up to 21 and 25% of the SAT variance in the autumn (SON) and winter (DJF), respectively (Łupikasza and Niedźwiedź, 2019). Similar percentages of SAT variance in winter over the Atlantic Arctic (22–27%) were explained by weather regimes in the period 1951–2014 (Champagne *et al.*, 2019). The meridional circulation, specifically the southern transport of warm and moist air into the Arctic, leads to more efficient absorption of long-wave radiation, not only at the surface, but also at the higher levels of troposphere (Graversen *et al.*, 2014). Although the NAO has been significantly correlated with SAT in some regions of the Arctic and in some seasons during the last decades, it cannot explain the rapid Arctic warming from 1920 because the NAO at that time had an opposite trend direction and remained close to the average climate condition for several decades (Przybylak, 2000; Bengtsson *et al.*, 2004; Wood and Overland, 2010).

Atmospheric circulation continues to contribute to contemporary climate warming in the Arctic (hereinafter CAW) (Przybylak, 2000, 2002; Overland and Wang, 2010; Fettweis *et al.*, 2011; Overland *et al.*, 2012; Hanna *et al.*, 2013, 2018; Bezeau *et al.*, 2015; Isaksen *et al.*, 2016; Ding *et al.*, 2017; Huang *et al.*, 2017). However, the relationship between the SAT and atmospheric circulation is currently modified by the dominant impact of greenhouse enhanced warming, resulting in generally warmer

air masses of all types (Isaksen *et al.*, 2016) and enhanced feedback mechanisms (Johannessen *et al.*, 2016; Ding *et al.*, 2017; Łupikasza and Niedźwiedź, 2019) which intensity depends on the local conditions (Yamanouchi, 2011). This observation is supported by weaker meridional circulation during the CAW which was a dominating pattern during the ETCAW (Overland *et al.*, 2008; Łupikasza and Niedźwiedź, 2019). A different role of atmospheric circulation for the two warming events namely, the ETCAW and the CAW, has also been suggested by Wegmann *et al.* (2017) based on different vertical distributions of maximum temperature anomalies currently at the surface but in the mid-troposphere during the ETCAW.

The regional and seasonal appearance of the ETCAW (Johannessen *et al.*, 2004; Overland *et al.*, 2004; Wegmann *et al.*, 2018; Łupikasza and Niedźwiedź, 2019) suggests the contribution of regional-scale determinants of climate variability that overlap or modify and complicate the understanding of the impact of large-scale factors. Moreover, Bengtsson *et al.* (2004) recommended that in the case of regional anomalies, the role of atmospheric and ocean circulation must be considered. These facts motivated us to check the impact of regional atmospheric circulation on Svalbard SAT. Our research area was selected based on existing studies that imply the crucial role of the atmospheric circulation over the Barents Sea (Bengtsson *et al.*, 2004; Polyakov *et al.*, 2010; Chen *et al.*, 2013; Suo *et al.*, 2013; Beitsch *et al.*, 2014; Johannessen *et al.*, 2016; Walsh *et al.*, 2017; Wang *et al.*, 2019) and the Greenland Sea (Ogi *et al.*, 2016; Walsh *et al.*, 2017; Champagne *et al.*, 2019) on the variability and change in the SAT in the Atlantic-Arctic. This study, which is based on station data, is important because most of the knowledge on historical Arctic warming comes from model projections (Tokinaga *et al.*, 2017).

In summary, our study seeks to explore the impact of the regional circulation over the four selected areas in the vicinity of Svalbard (Greenland and Norwegian Sea) on Svalbard's SAT variability for the period 1920–2018, with a particular focus on the two warmest sub-periods within the instrumental measurements namely, the ETCAW and CAW. We also examined whether there were any spatial and temporal differences in these relations by comparing the ETCAW and CAW sub-periods with the Cold Arctic sub-Period (CAP) that separated them. Our study is the first to present the regional variability in the impact of atmospheric circulation on SAT in the Atlantic sector of the Arctic, with a particular focus on warm and cold sub-periods. This article is organized as follows: Section 2 presents the data and methods used in the article, including the procedure for calculating the regional circulation indices. Section 3.1 is devoted to

changes in SAT regimes characterized by moving 30-year averages of seasonal SAT to select the natural warmest and coolest periods in the series at Svalbard, represented by the Svalbard Airport and Bjørnøya stations. This subsection also discusses variability in circulation indices for the entire 1920–2018 period and changes in their average values between the selected warm (ETCAW, CAW) and cold (CAP) sub-periods. Section 3.2 discusses the strength and statistical significance of the relation between the circulation indices in four regional circulation areas and SAT over Svalbard. Temporal variability in the pattern of regression between SAT and circulation indices for the selected Regional Circulation Areas (RCAs, see Section 2 for details), is recognized in Section 3.3. Summary and discussion followed by Conclusions are included in Sections 4 and 5, respectively.

2 | DATA AND METHODS

A new composite series of daily SAT for Svalbard Airport station (SA) (Nordli *et al.*, 2020) and daily SAT from Bjørnøya station (Bj) were used to recognize the impact of atmospheric circulation on the changes and variability in the SAT (2 m above ground) over Svalbard for 1920–2018. Sea-level pressure from the NOAA-CIRES Twentieth Century Reanalysis Version 2c (20CRv2c) (Compo *et al.*, 2011) for the period 1920–2014 (latitude–longitude grid resolution $2.0^\circ \times 2.0^\circ$) and the National Centers for Environmental Prediction/National Center for Atmospheric Research (NCEP/NCAR) reanalysis (Kalnay *et al.*, 1996) for the period 2015–2018 (latitude–longitude grid resolution $2.5^\circ \times 2.5^\circ$) were used to calculate circulation types and three related circulation indices: zonal circulation index (Wi), meridional circulation index (Si), and cyclonicity index (Ci). In the case of NCEP/NCAR data that have different spatial distribution compared to NOAA-CIRES, before calculating the circulation indices for this extra period, sea-level pressure was interpolated for the nodal and central points that are shown in Figure 1. The indices deliver information on the frequency of air advection (Wi, Si) from the main (S/N, W/E) and intermediate directions (NE, SE, etc.) and dominant type of baric systems (Ci). The indices were calculated for four neighbouring areas, hereinafter referred to as 'Regional Circulation Areas' (RCAs). The RCAs cover the following domains (Figure 1): (1) RCA_{Sp} –Spitsbergen: $76\text{--}80^\circ\text{N}$ and $10\text{--}30^\circ\text{E}$; (2) RCA_{Bj} –Bjørnøya: the area between Spitsbergen and Scandinavian Peninsula: $72\text{--}76^\circ\text{N}$ and $10\text{--}30^\circ\text{E}$; (3) RCA_{GSN} , the northern part of the Greenland Sea: $76\text{--}80^\circ\text{N}$ and $10^\circ\text{W}\text{--}10^\circ\text{E}$; and (4) RCA_{GSS} , the southern part of Greenland Sea: $72\text{--}76^\circ\text{N}$ and $10^\circ\text{W}\text{--}10^\circ\text{E}$. The selected RCAs are

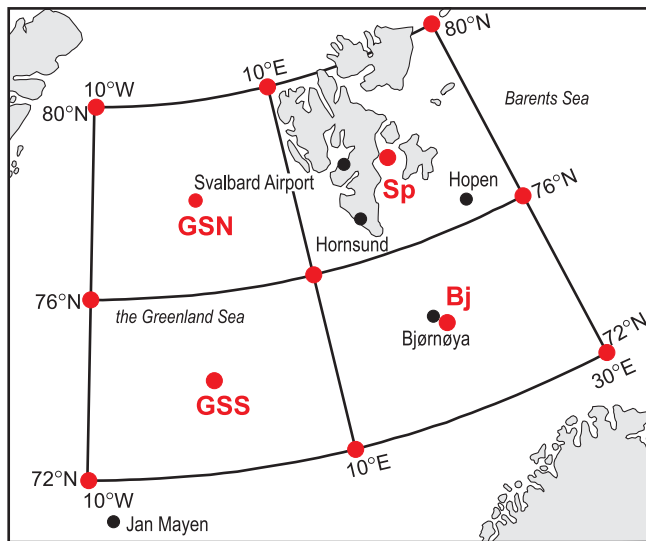


FIGURE 1 Location of the RCAs: RCA_{Sp} , Spitsbergen; RCA_{Bj} , Bjørnøya; RCA_{GSN} , northern part of the Greenland Sea; RCA_{GSS} , southern part of the Greenland Sea; small dots, meteorological stations; big dots, nodal points, and central points [Colour figure can be viewed at wileyonlinelibrary.com]

crucial for the climate of the entire Arctic due to low-pressure systems that frequently pass these areas (Greenland Sea or Barents Sea) and bring warm and humid air to the Arctic from lower latitudes (Serreze and Barry, 1988; Zhang *et al.*, 2004; Tsukernik *et al.*, 2007; Turner and Marshall, 2011); intensive inflow of warm Atlantic Waters to the Arctic Ocean within the West Spitsbergen Current (Piechura and Walczowski, 2009). Moreover, a rapid deepening of lows and redevelopment of extratropical systems that migrate from the south, takes place in the region because of strong baroclinity across the ice-sea margin (Serreze *et al.*, 1997). As a result, changes in regional atmospheric circulation over the RCAs may influence SAT behaviour over Svalbard more directly than macroscale circulation. In order to verify this, circulation indices for each RCA were calculated similar to those proposed by Murray and Lewis (1966) and Niedźwiedz (1993, 2013), however, the indices were simplified because of the automation of the calculation procedure. First, gradients of air pressure (ΔP) were calculated as differences between the average air pressure (P) for bordering parallels in the case of W_i , or for bordering meridians in the case of S_i . The formulas for calculating W_i and S_i for RCA_{Sp} are presented (with example co-ordinates) in Equations (1) and (2), respectively.

$$\begin{aligned} \Delta P_{W-E} &= P_{76N} - P_{80N}, \text{ where } P_{76N} = \\ &= (P_{76N10E} + P_{76N30E})/2 \text{ and } P_{80N} = \\ &= (P_{80N10E} + P_{80N30E})/2 \end{aligned} \quad (1)$$

$$\begin{aligned} \Delta P_{S-N} &= P_{30E} - P_{10E}, \text{ where } P_{30E} = \\ &= (P_{80N30E} + P_{76N30E})/2 \text{ and } P_{10E} = \\ &= (P_{80N10E} + P_{76N10E})/2 \end{aligned} \quad (2)$$

The ΔP_{W-E} and ΔP_{S-N} gradients inform on the intensity and direction of air advection according to the following criteria:

- $\Delta P_{W-E} > +2$ hPa \rightarrow air advection from western sector (W)
- $\Delta P_{W-E} < -2$ hPa \rightarrow air advection from eastern sector (E)
- $\Delta P_{S-N} > +2$ hPa \rightarrow air advection from southern sector (S)
- $\Delta P_{S-N} < -2$ hPa \rightarrow air advection from northern sector (N)

or the research area, the difference in sea-level pressure of ≤ 2 hPa refers to geostrophic wind speed $< 2.0\text{--}2.5$ $\text{m}\cdot\text{s}^{-1}$ depending on the latitude. Therefore, the gradients between -2 hPa $\leq \Delta P \leq 2$ hPa were counted as non-advective conditions and marked '0'.

The type of baric centre was classified based on the sea-level pressure in the central point of each RCA (RCA_{Sp} , RCA_{Bj} , RCA_{GSN} , RCA_{GSS} , see Figure 1), referring to the normal pressure of 1,013 hPa as a threshold value between the low and high-pressure systems that is, $>1,013$ hPa for anticyclonic situations (a) and $<1,013$ hPa for cyclonic situations (c).

Next, we identified the direction of air advection: 'W', '0', or 'E' for zonal flow and 'S', '0', or 'N' for meridional flow, and 'a' or 'c' for type of baric centre, and used them to recognize the circulation type for each day of the research period. As a result, 18 circulation types were created, including nine anticyclonic and nine cyclonic types, as shown in Table 1. The 0a and 0c circulation types denote non-advective situations that is, situations with weak airflow (-2 hPa $\leq \Delta P \leq 2$ hPa).

Based on the distinguished circulation types, three circulation indices (W_i , S_i , and C_i) were calculated by attributing a particular number of score (+2, +1, -1, or -2) to each circulation type depending on the direction of air advection (W_i , S_i) or type of baric centre (C_i), as follows:

- W_i : +2 for W, +1 for NW and SW, -2 for E, -1 for NE and SE. Positive values of W_i indicate a predominance of air advection from the W sector, while negative values indicate an easterly airflow.
- S_i : +2 for S, +1 for SW and SE, -2 for N, -1 for NW and NE. Positive values of S_i indicate a predominance of southern advection, while negative ones point to a northerly airflow.

TABLE 1 Classification of the circulation types (CT) based on the zonal (W–0–E) and meridional (S–0–N) directions of air advection and type of baric centre

Anticyclonic circulation types				Cyclonic circulation types			
S–0–N	W–0–E	a/c	CT	S–0–N	W–0–E	a–c	CT
N	0	a	Na	N	0	c	Nc
N	E	a	NEa	N	E	c	NEc
0	E	a	Ea	0	E	c	Ec
S	E	a	SEa	S	E	c	Sec
S	0	a	Sa	S	0	c	Sc
S	W	a	SWa	S	W	c	SWc
0	W	a	Wa	0	W	c	Wc
N	W	a	NWa	N	W	c	NWc
0	0	a	0a	0	0	c	0c

Abbreviations: a, anticyclonic; c, cyclonic.

- *Ci*: +1 for 0c, for Nc, NEc, Ec, SEc, Sc, SWc, Wc, NWc; –1 for Na, NEa, Ea, SEa, Sa, SWa, Wa, NWa, and 0a. The *Ci* focuses on the frequency of cyclonic and anticyclonic conditions. Positive values of *Ci* indicate a predominance of cyclonic types, while negative values indicate a predominance of anticyclonic types.

The scores were then summarized on a monthly basis and expressed as percentages with 100% being the potential maximum number of scores in a month, which is 30 or 60 (30×2), 32 or 62 (31×2), and 28 or 56 (28×2) depending on the month; in the case of *Si* and *Wi* the number of days in a month was multiplied by 2 because the maximum score for a day is 2. Theoretically, the index values may range from +100% to –100%, where +100% means southern (in the case of *Si*) or western (in the case of *Wi*) advection of air masses during the entire month. A value of –100% means an air advection from the opposite sector (i.e., northern for *Si* or eastern for *Wi*).

The strengths of relations between the regional circulation over various RCAs and the SAT over Svalbard were identified with multiple regression coefficients that were calculated for the entire research period 1920–2018 (for series with trends and de-trended with the second polynomial), warmest 30-year sub-periods (ETCAW and CAW), and for the CAP that occurs between them. In multiple regression, SAT was used as the dependent variable, while all the circulation indices (*Si*, *Wi*, and *Ci*) were used as explanatory variables. All mentioned 30-year sub-periods were selected by detailed analysis of the moving 30-year averages of seasonal SATs and they are, except for the CAW, represented by various 30-year sub-periods depending on the season (Table 2, see Section 3.1 for more details). Trends in regional circulation indices were calculated using the least-squares method (Cantrell, 2008; Wilks, 2019). The statistical significance of differences in mean seasonal SAT and circulation

indices between ETCAW, CAP, and CAW was tested with Student's *t*-test (Wold, 1995; Bastien *et al.*, 2005). Threshold of $\alpha = .05$ was adopted to identify significant cases.

3 | RESULTS

3.1 | Changes in air temperature and regional circulation indices

3.1.1 | Air temperature

The 30-year moving averages shown in Figure 2 represent changes in SAT regimes with reduced short-term variability, enabling the climatological WMO normal periods to be compared against the naturally selected warmest and coldest 30-year sub-periods. There was a gradual warming in the consecutive 30-year sub-periods from 1920 until the beginning of the 1930s at both the stations (except for DJF in Bj station and JJA in the SA station), that showed a peak in 1931–1960 (MAM, JJA), 1933–1962 (SON), or 1929–1958 (DJF) (depending on the season). In MAM and JJA those 30-year sub-periods were 0.1°C to 0.3°C cooler than the long-term mean (). In SON, the warmest 30-year sub-periods marking the peak of ETCAW were 0.9°C (Svalbard Airport) and 0.3°C (Bjørnøya) warmer than the long-term averages calculated for these stations, while in DJF they were warmer by 1.6 and 0.5°C, respectively. The latest sub-period of clear gradual warming started at the beginning of the 1960s, except for SON, when the warming began in the mid-1960s. From then onwards, the 30-year SATs rose, and in the last 30-year sub-period (1989–2018) the temperatures were higher than the long-term average by a maximum of 2.5°C (SA station) and 1.3°C (Bj station) in DJF. In the coldest 30-year sub-periods, the seasonal

TABLE 2 Warm and cold 30-year sub-periods representing the Early Twentieth Century Arctic Warming (ETCAW), Cold Arctic Period (CAP), and Contemporary Arctic Warming (CAW)

Sub-period	MAM	JJA	SON	DJF
ETCAW	1931–1960	1931–1960	1933–1962	1929–1958
CAP	1961–1990	1961–1990	1966–1995	1959–1988
CAW	1989–2018	1989–2018	1989–2018	1989–2018

SATs dropped, and they were lower than the long-term average by 0.5°C (JJA) to 1.8°C (DJF) at the Svalbard Airport and by 0.4°C (SON) to 1.9°C (DJF) at the Bjørnøya station. Except for summer, the average SAT at Bjørnøya station was several degrees higher than at Svalbard Airport station, which has more continental climate conditions.

In the next part of this article, we focus on the warmest 30-year sub-periods representing the ETCAW and CAW and the coldest sub-period (CAP) between the two warmest episodes; all the sub-periods are underlined in Figure 2 and presented in Table 2. In the case of MAM and JJA, we decided to select the 1961–1990 sub-period to represent the CAP to avoid its overlap with the ETCAW, which would prohibit the testing of the differences in the averages of SAT and circulation indices. The average SAT for the selected 30-year sub-periods representing the ETCAW, CAW, and CAP are presented in Table 3. The SAT during the ETCAW was significantly higher than during the CAP only in SON and DJF. In MAM and JJA, the ETCAW was significantly colder than the CAW, but no compelling differences in SAT between these periods were found in SON and DJF. To summarize, on Svalbard, in the early 20th-century, a significant warming occurred in SON and DJF; this warming was more intense at the Svalbard Airport station than at the Bjørnøya station.

3.1.2 | Circulation indices

The average seasonal circulation indices for individual RCAs are presented in Figure 3. The W_i describes the dominating easterlies in the polar regions with their highest frequency in DJF. In the northern RCAs, the easterlies are more frequent than in the southern RCAs. The S_i shows clear regional differentiation. The eastern RCAs experience a dominance of southerly advection, while northerly advection prevails over the western RCAs, which is linked to the eastern part of the Greenland High. Such diversity may produce various impacts of RCAs on long-term variability in SAT. Seasonal diversification also concerns the frequency of the cyclonic conditions, which clearly prevails in SON and DJF (Figure 3). In MAM, all RCAs were more frequently

under the influence of anticyclones than cyclones. Previous studies on the frequency of circulation types over Hornsund indicated that May is the month with the greatest frequency of anticyclonic circulation (Niedźwiedz, 1993, 2013). In JJA, the difference between the frequency of the anticyclonic and cyclonic types was minor, 1–10% depending on the RCA.

Temporal variabilities in the circulation indices describing the frequency of air advection or cyclonic/anticyclonic conditions for each season and for each RCA are presented in Figures 4 and 5. The horizontal lines show the 30-year-average index values for the ETCAW, CAP, and CAW, which are also shown in Table 4. Linear trends for seasonal circulation indices are presented in Table 5.

3.1.3 | Spring (MAM)

Trends in circulation indices were most prominent in spring. In each RCA, there was an increase in the frequency of cyclonic conditions for this season, particularly over RCA_{Sp} (3.3% per decade). The C_i averages for the selected 30-year periods increased within the research period, independent of whether the period was cold or warm. Significant difference in average C_i was found between the ETCAW and CAW in all the RCAs (Figure 4, Table 4). Significant positive trends were also found in W_i over most RCAs except for RCA_{GSS} , which translates into westerlies more frequent at over one-third or less than one-fourth the rate of C_i . Moreover, significant differences in W_i between the ETCAW and CAW were found in the eastern RCAs. A significant S_i trend at a rate of -1.1% per decade that was found in MAM, suggested the lowering frequency of the southerly advection, but only over RCA_{Sp} (Table 5).

3.1.4 | Summer (JJA)

Trends in summer S_i were negative, but higher frequency of air advection from the N sector was statistically significant only in the eastern RCAs (Table 5). The S_i averages did not differ significantly between the 30-year sub-periods. However, in each RCA, the S_i values decreased rapidly

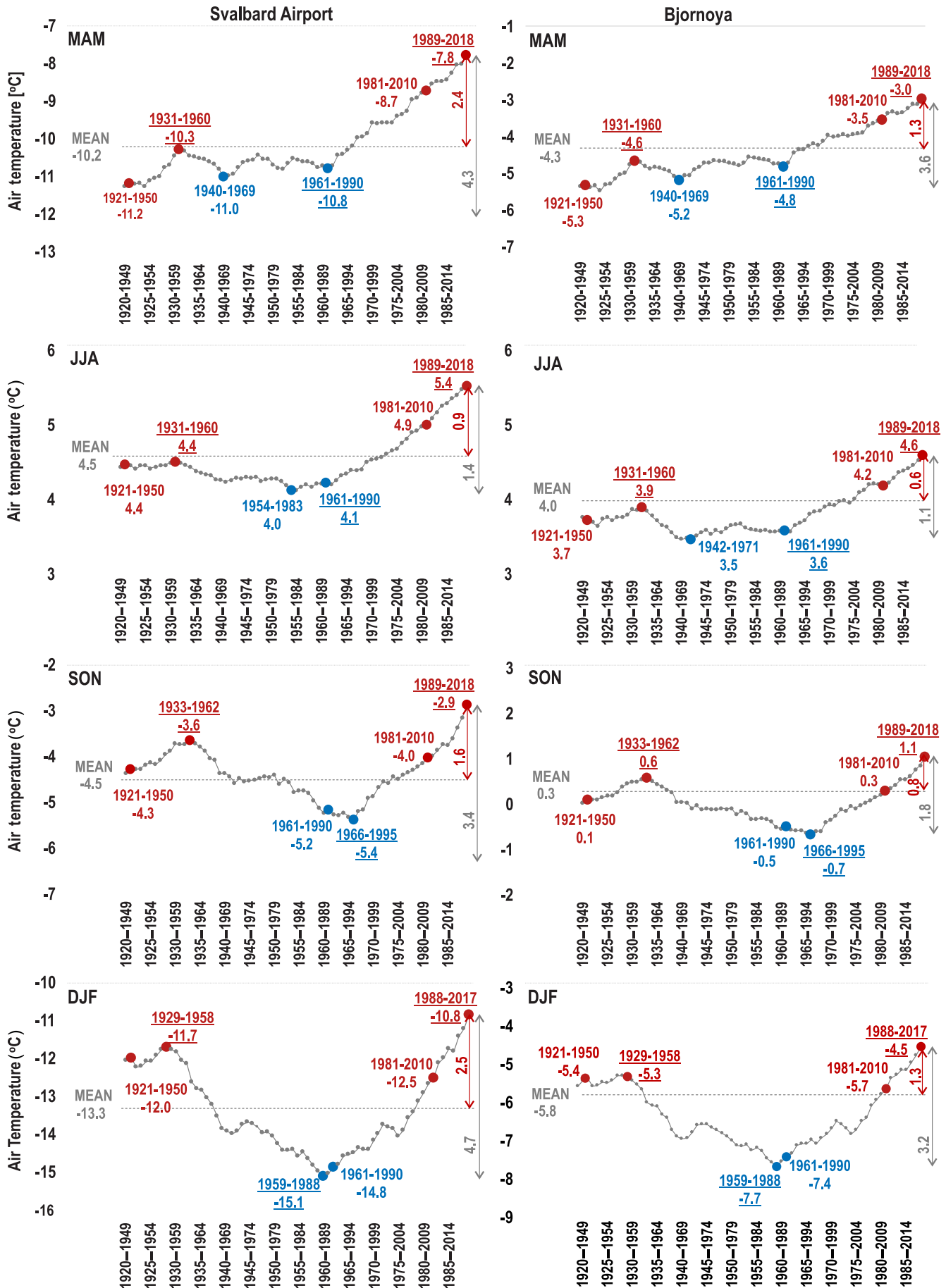


FIGURE 2 Legend on next page.

TABLE 3 Average air temperature (°C) for the ETCAW, CAW, and CAP at Bjørnøya (Bj) and Svalbard Airport (SA) stations and related differences in averages between these periods

Period/station	MAM		JJA		SON		DJF	
	Bj	SA	Bj	SA	Bj	SA	Bj	SA
ETCAW	-4.6	-10.3	3.9	4.4	0.6	-3.6	-5.3	-11.8
CAP	-4.8	-10.8	3.6	4.1	-0.7	-5.4	-7.7	-15.1
CAW	-3.0	-7.8	4.6	5.4	1.1	-2.9	-4.5	-10.8
ETCAW-CAP	0.2	0.5	0.3	0.2	1.2***	1.7***	2.3***	3.3***
ETCAW-CAW	-1.7***	-2.5***	-0.7***	-1.0***	-0.5	-0.8	-0.8	-0.9

Note: Statistical significance: * ≤ 0.05 , ** ≤ 0.01 , *** ≤ 0.001 , significant cases are bolded.

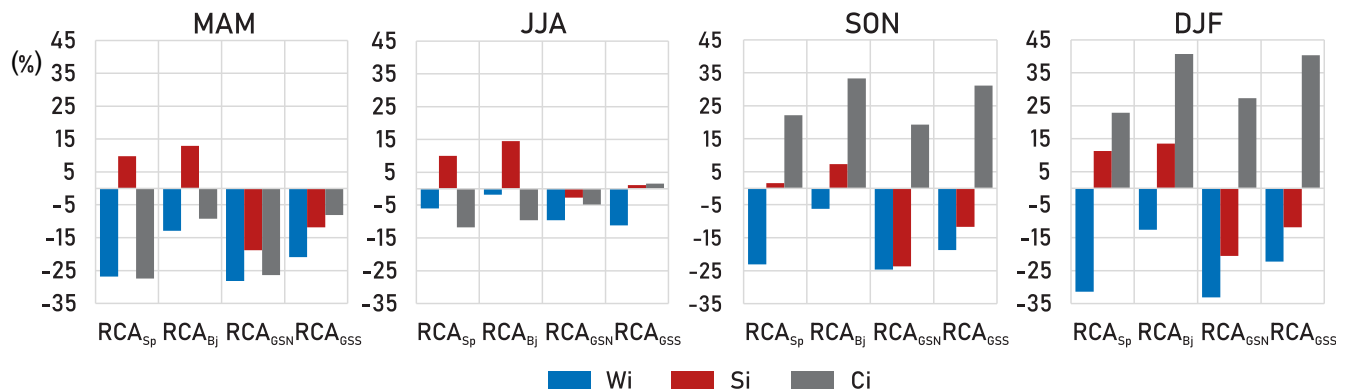


FIGURE 3 Average seasonal circulation indices for RCAs 1920–2018 (configuration of the RCAs is shown in Figure 1) [Colour figure can be viewed at wileyonlinelibrary.com]

during the ETCAW (between 1930s and 1955) (Figure 4). The frequency of cyclonic conditions increased in summer in each RCA, but insignificantly (Table 5). The multi-decadal changes in summer Ci were more important. In the southern part of the research area the frequency of cyclonic conditions was significantly higher in the CAP than in the ETCAW. This contradicts with the previous findings that cyclonic activity intensified during warm periods (Wood and Overland, 2010), however, it is important that JJA warming was weak; the difference in the summer SAT between the ETCAW and the CAP was insignificant (Table 3). Moreover, long-term trends in Ci were positive, though insignificant. In JJA, three RCAs exhibited significant increase in the Wi between the ETCAW and CAW (Tables 4 and 5). Despite the increase, the index value remained negative (domination

of easterly air advection) with the exception of RCA_{Sp} , where westerly advection slightly dominated easterly advection during the CAW (Table 4). In the eastern RCAs, Wi decreased during the ETCAW (more frequent eastern advection) and increased during the CAP (more frequent western advection) (Figure 3).

3.1.5 | Autumn (SON) and winter (DJF)

In SON and DJF when the ETCAW was clearly marked in the chronological series of SAT, the circulation indices did not exhibit significant long-term trends except for single cases limited to DJF, such as Wi and Si in northern RCAs (Table 5). Although linear trends were insignificant

FIGURE 2 Thirty-year moving averages of seasonal air temperatures (SAT) in the period 1920–2018 for Svalbard Airport and Bjørnøya stations. Selected WMO normal periods and the warmest and coldest 30-year sub-periods representing the ETCAW, CAW, and CAP are marked with dots. The underlined sub-periods were selected for further analysis of relationships between SAT and circulation indices. dots, coldest periods and warmest periods. Grey dashed horizontal line represents the average SAT for the long-term period of 1920–2018. Shorter vertical arrows, departure of mean SAT during the CAW from long-term mean; longer vertical arrows, the entire range of SAT variability in the research period. [Correction added on 22 February 2021, after first online publication: In the original published version, figures 2 and 3 were mistakenly interchanged. This version corrects the error.] [Colour figure can be viewed at wileyonlinelibrary.com]

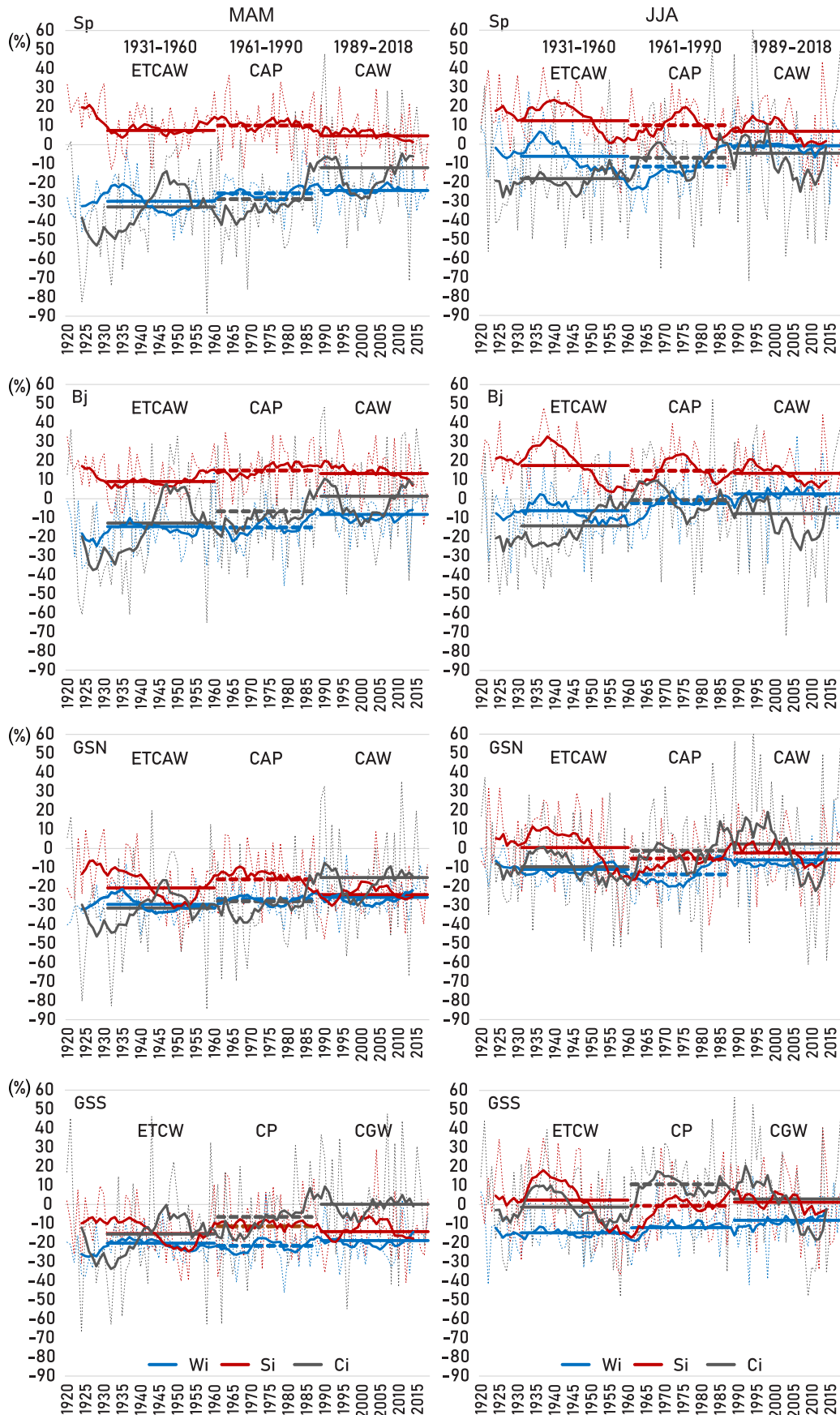


FIGURE 4 Legend on next page.

in SON, the multi-decadal changes in average Si between the ETCAW and the CAP were significant for all the RCAs, indicating more frequent air advection from the southern sector during the ETCAW. This rise in the frequency was approximately twice as large over the Greenland Sea as over the eastern part of the research area (Table 4). In SON, the difference in mean Wi between the ETCAW and the CAP was also significant, but only over the RCA_{Bj} , indicating more frequent eastern advection in the CAP than in the warm periods. These may also be noted in other RCAs but with no statistical significance. Significant changes in both SON circulation indices and SAT between the ETCAW and CAP (Tables 3 and 4) show that during this season atmospheric circulation might have driven the most multi-decadal changes in SAT. In DJF, when the difference in SAT between the ETCAW and CAP was the largest at both stations, significant changes in regional atmospheric circulation were less evident than those observed in SON. Significant differences between the ETCAW and CAP were only found for Si over RCA_{Sp} , where southerly advection during the ETCAW was more frequent than in the CAP. In DJF, significant increase in the frequency of cyclonic activity during the CAW (compared to the ETCAW) was also found over the Greenland Sea (RCA_{GSS} and RCA_{GSN}), although no significant difference in SAT was found between these periods in winter (Table 4).

In summary, in SON and DJF, when the ETCAW was clearly warmer than the following CAP, trends in regional circulation indices were much weaker than in JJA and MAM, and they were mostly insignificant. In SON, significant increase in the frequency of S advection contributed to the ETCAW. The impact of regional circulation indices on winter ETCAW seems to be limited to RCA_{Sp} , where the frequency of S advection also increased during the ETCAW. In DJF, the negative long-term linear trend (1920–2018) in Si over RCA_{Sp} was also significant. In the next section, the strength of the joint impact of regional circulation indices on SAT is quantified, and the RCA that has the greatest impact on the variability of the SAT is identified.

3.2 | Relationship between air temperature over Svalbard and circulation indices over various RCAs in Atlantic sector of Arctic

The impact of regional circulation on SAT variability was studied for each meteorological season (MAM, JJA,

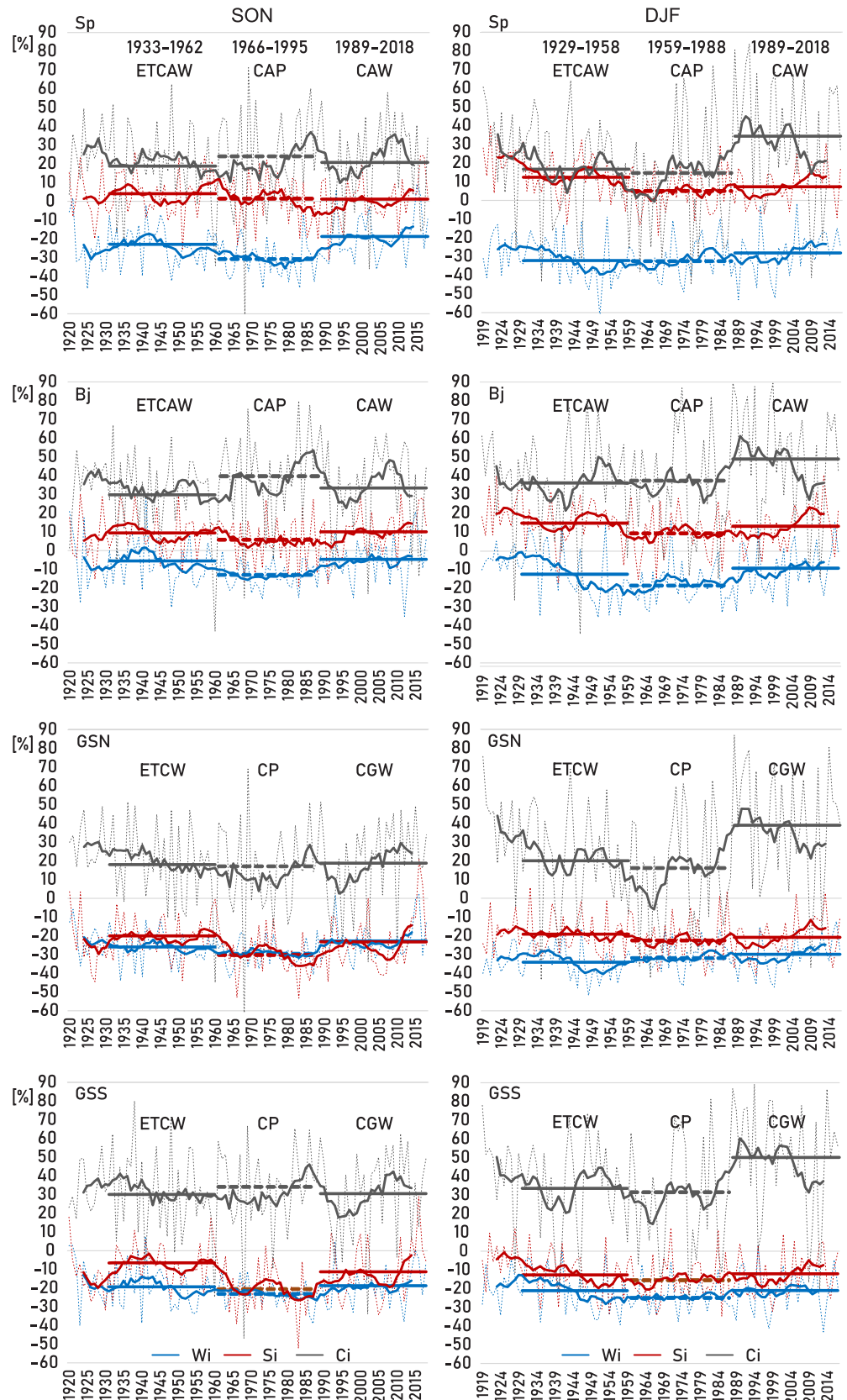
SON, and DJF) for the entire research period (1920–2018) with multiple regression (Tables 6 and 7). We calculated the regression using the original series that is, with trends (if existing, referred to as ‘original series’) and also de-trended series to find the possible effect that trends in both parameters had on their relationships.

Considering the original series, the relations between SAT and circulation indexes show various patterns depending on season and station. Generally, atmospheric circulation over all RCAs significantly contributed to the variability in SAT at both stations. This impact was stronger at Bjørnøya station than at Svalbard Airport station. Multiple regression showed that the circulation indices, together, explained a maximum of 29% (JJA) to 57% (SON) of variance in the Bjørnøya SAT and 29–51% of variance in Svalbard Airport SAT (Tables 6 and 7). The summer SAT at Svalbard Airport was not related to any of the regional circulation indices in any RCA. At both stations, the highest percentage of variance in SAT was explained by atmospheric circulation over RCA_{Bj} or RCA_{Sp} depending on season, with the maximum coefficients of determination in SON. Atmospheric circulation over RCA_{Bj} drove the variability in SAT in most seasons, except for summer at Bjørnøya station and for MAM and DJF at the Svalbard Airport station (Tables 6 and 7). Spatial variability in the strength of the relationships between the indices and SAT, assessed as the difference between the maximum and minimum coefficient of determination for RCAs during each season, was clearly higher in SON and DJF than that in MAM and JJA, particularly for Bjørnøya station. With regards to particular circulation indices, the multiple regression indicated that the Si index had the strongest impact on SAT at both stations in SON and DJF and over every RCAs. The situation is interesting in spring when the highest regression coefficients are characteristic of Wi over RCA_{Bj} and Ci over all other regional circulation areas (Sp, GSN, and GSS). Significant differences in mean Wi between the ETCAW and the current warm period over RCA_{Bj} and in mean Si index between the ETCAW and cold period over all of the RCAs in SON (see previous section) indicate the contribution of atmospheric circulation to changes in mean SAT between these periods.

Trends in the chronological series did not markedly influence the relationships between the SAT and circulation indices, except for those observed in the summer at

FIGURE 4 Long-term variability in circulation indices in the period 1920–2018 for spring and summer. Thin dotted lines, year-to-year index values; thick solid lines, 7-year moving averages; horizontal solid lines represents 30-year average indices for ETCAW, and CAW; horizontal dashed lines represents the CAP [Colour figure can be viewed at wileyonlinelibrary.com]

FIGURE 5 Long-term variability in circulation indices in the period 1920–2018 for autumn and winter. Thin dotted lines, year-to-year index values; thick solid lines, 7-year moving averages; horizontal solid lines represents 30-year average indices for ETCAW, and CAW; horizontal dashed lines represents the CAP [Colour figure can be viewed at wileyonlinelibrary.com]



Svalbard Airport station, where trends reduced the regression between the variables to an insignificant level (Table 6). At Svalbard Airport, the de-trended data shows

significant relationships between summer SAT and Si. In other seasons, the difference in coefficients of determination between the original and de-trended series did not

TABLE 4 Average values of seasonal circulation indices for the warm (ETCAW, CAW) and cold (CAP) periods and related differences in means with statistical significance

Period/season	MAM			JJA			SON			DJF		
	Wi	Si	Ci	Wi	Si	Ci	Wi	Si	Ci	Wi	Si	Ci
<i>RCA_{Sp}</i>												
ETCAW	-29.7	7.5	-32.6	-6.3	12.4	-18.0	-23.4	5.3	18.8	-32.5	12.8	18.9
CAP	-25.5	10.1	-28.6	-11.7	10.0	-7.1	-28.4	-2.4	21.2	-31.5	4.9	12.7
CAW	-24.0	4.7	-12.1	-0.8	6.8	-4.7	-18.7	1.2	20.7	-28.1	7.3	30.8
ETCAW-CAP	-4.3	-2.5	-4.0	5.5	2.4	-10.9	5.1	<u>7.7*</u>	-2.4	-1.0	<u>7.9**</u>	6.2
ETCAW-CAW	-5.8*	2.9	-20.5**	-5.5	5.6	-13.3	-4.6	4.1	-1.9	-4.4	5.5	-11.9
<i>RCA_{Bj}</i>												
ETCAW	-14.7	9.0	-12.8	-6.2	17.5	-14.2	-5.4	10.1	29.4	-11.9	15.4	37.7
CAP	-15.1	14.8	-6.6	-2.2	14.8	-0.6	-11.8	3.2	40.3	-17.6	9.4	34.5
CAW	-8.3	13.2	-1.3	2.6	13.4	-7.0	-4.7	10.0	33.4	-9.0	13.2	47.3
ETCAW-CAP	0.4	-5.8	-6.2	-3.9	2.6	-13.6*	<u>6.4*</u>	<u>6.9*</u>	-10.9	5.7	6.0	3.2
ETCAW-CAW	-6.3*	-4.2	-14.1*	-8.7*	4.0	-7.2	-0.7	0.1	-4.0	-2.9	2.3	-9.6
<i>RCA_{GSN}</i>												
ETCAW	-29.4	-20.7	-18.9	-11.0	0.4	-9.7	-26.3	-19.5	18.2	-34.5	-19.7	21.8
CAP	-26.6	-16.2	-17.2	-13.7	-5.4	-1.3	-27.2	-30.4	14.3	-31.4	-22.1	14.5
CAW	-25.7	-24.2	-9.4	-6.1	-2.4	-2.3	-22.7	-23.2	18.8	-29.9	-20.8	37.2
ETCAW-CAP	-2.8	-4.5	-3.6	2.7	5.8	-8.4	0.9	<u>11.0***</u>	3.9	-3.1	2.4	7.3
ETCAW-CAW	-3.6	3.5	-16.0*	-4.9*	2.7	-12.0	-3.6	3.7	-0.6	-4.5	1.1	-15.4*
<i>RCA_{GSS}</i>												
ETCAW	-20.3	-15.3	-15.5	-14.8	2.4	-1.3	-19.0	-6.1	30.4	-21.0	-12.7	35.2
CAP	-21.7	-11.4	-6.5	-12.1	-0.6	10.7	-22.6	-20.5	29.2	-24.5	-15.3	29.2
CAW	-18.9	-14.2	-0.14	-8.2	1.3	1.7	-18.7	-11.3	30.5	-21.0	-12.1	50.9
ETCAW-CAP	1.4	-3.9	-9.0	-2.7	3.1	-12.0*	3.6	<u>14.4***</u>	1.2	3.5	2.7	6.0
ETCAW-CAW	-1.4	-1.0	-15.6*	-6.7*	1.1	-3.0	-0.3	5.2	-0.1	0.1	-0.6	-15.7*

Note: Statistical significance: * ≤ 0.05 , ** ≤ 0.01 , *** ≤ 0.001 , significant cases are bolded, italic—negative differences; underlined italic—positive differences.

TABLE 5 Linear trends (change in index value per decade) in regional circulation indices in the period 1920–2018

RCA	MAM			JJA			SON			DJF		
	Wi	Si	Ci	Wi	Si	Ci	Wi	Si	Ci	Wi	Si	Ci
Sp	+0.8*	-1.1*	+3.3***	+0.4	-1.6**	+1.9	+0.5	-0.3	-0.1	+0.2	-1.4**	+1.0
Bj	+1.2**	+0.2	+2.7**	+1.2*	-1.3**	+1.5	-0.1	+0.1	+0.2	-0.3	-0.5	+1.1
GSN	+0.6*	-1.0	+2.1*	+0.7*	-1.0	+1.2	+0.2	-0.4	-0.6	+0.6*	-0.2	+0.8
GSS	+0.5	-0.2	+2.4**	+1.0*	-0.6	+0.8	-0.3	-0.4	-0.1	-0.3	-0.5	+1.0

Note: Statistical significance: * ≤ 0.05 , ** ≤ 0.01 , *** ≤ 0.001 , significant cases are bolded.

exceed 9% in most cases (Tables 5 and 6), but the direction of the impact (strengthening/weakening after detrending) depended on season and also on RCA. In MAM, trends strengthened the relation at both stations, while in SON the effect was inverted except for RCA_{Bj} . In DJF, trends increased the coefficients of determination at

Bjørnøya station and decreased it at Svalbard Airport station, with the exception of RCA_{GSN} . This may result from various seasonally dependent factors playing a dominant role in shaping the long-term variability of SAT. In summer, these factors are of more local character than regional circulation (this will be extended in Section 4).

TABLE 6 Statistics for multiple regression between seasonal air temperature at Svalbard Airport station and circulation indices (Wi, Si, and Ci) for various RCAs, 1920–2018

Season	Series with trends	RCA	Regression coefficients for circulation indices			R2 [%]
			Wi	Si	Ci	
MAM	Sp		.275 **	.146	.414 ***	27 ***
	Bj		.394 ***	.235 **	.174	29 ***
	GSN		.255 **	.079	.444 ***	24 ***
	GSS		.295 *	.048	.317 ***	22 ***
JJA	Sp		.198	.022	-.225 *	7
	Bj		-.034	.030	-.145	3
	GSN		.137	.245	-.104	8
	GSS		-.009	.203	-.137	5
SON	Sp		.282 ***	.652 ***	.078	51 ***
	Bj		.172 *	.640 ***	-.034	49 ***
	GSN		-.087	.557 ***	.304 ***	36 ***
	GSS		.013	.550 ***	.311 ***	34 ***
DJF	Sp		.269 **	.487 ***	.273 **	39 ***
	Bj		.359 ***	.488 ***	.096	42 ***
	GSN		.097	.496 ***	.369 ***	35 ***
	GSS		.070	.399 ***	.021 *	21 ***
De-trended series						
MAM	Sp		.203 *	.282 **	.273 **	19 ***
	Bj		.305 **	.289 **	.074	21 ***
	GSN		.158	.179	.353 ***	15 **
	GSS		.260 **	.104	.203 *	14 **
JJA	Sp		-.011	.338 ***	-.239 *	22 ***
	Bj		-.347 ***	.330 ***	-.113	24 ***
	GSN		-.160	.372 ***	-.113	21 ***
	GSS		-.366 ***	.284 **	.011	19 ***
SON	Sp		.174 *	.711 ***	.053	54 ***
	Bj		.131	.665 ***	-.036	49 ***
	GSN		-.145	.594 ***	.316 ***	41 ***
	GSS		.018	.561 ***	.337 ***	35 ***
DJF	Sp		.245 **	.568 ***	.254 **	43 ***
	Bj		.373 **	.511 ***	.051	45 ***
	GSN		.069	.507 ***	.303 ***	30 ***
	GSS		.108	.378 ***	.128	19 ***

Note: R2, coefficient of determination for the multiple regression in %; p, statistical significance for the multiple regression; p, threshold of statistical significance: * ≤.05, ** ≤.01, *** ≤.001, italic underlined, highest R2; italic, lowest R2; significant cases are bolded.

The small differences in regression between the original and de-trended series may result from similar impacts of some climate change drivers (e.g., sea ice extend, human-induced changes) on the temporal changes in SAT and circulation indices or can indicate the significant causality between these variables.

3.3 | Circulation-based air temperature changes during ETCAW, CAW, and CAP in autumn and winter

The variability in SAT, as shown in the previous section, is significantly related to the frequency of cyclonic/

Season	RCA	Regression coefficients for circulation indices			R2[%]
		Wi Series with trends	Si	Ci	
MAM	Sp	.250 **	.290 ***	.449 ***	33 ***
	Bj	.417 ***	.358 ***	.178 *	<u>40 ***</u>
	GSN	.118	.221 *	.526 ***	29 ***
	GSS	.253 **	.189 *	.413 ***	32 ***
JJA	Sp	.450 ***	.262 **	.032	<u>29 ***</u>
	Bj	.306 **	.319 **	-.043	22 ***
	GSN	.168	.381 ***	.203 *	21 ***
	GSS	.197 *	.408 ***	.065	24 ***
SON	Sp	.261 ***	.671 ***	.163 *	52 ***
	Bj	.186 **	.705 ***	.050	<u>57 ***</u>
	GSN	-.153	.547 ***	.367 ***	39 ***
	GSS	-.021	.565 ***	.410 ***	40 ***
DJF	Sp	.182 *	.573 ***	.341 ***	45 ***
	Bj	.330 ***	.583 ***	.212 **	<u>51 ***</u>
	GSN	-.002	.493 ***	.450 ***	37 ***
	GSS	.047	.407 ***	.304 ***	25 ***
De-trended series					
MAM	Sp	.186 *	.409 ***	.325 ***	30 ***
	Bj	.352 ***	.412 ***	.106	<u>36 ***</u>
	GSN	.015	.312 ***	.443 ***	26 ***
	GSS	.220 *	.250 **	.338 ***	27 ***
JJA	Sp	.330 ***	.407 ***	.051	<u>31 ***</u>
	Bj	.201 *	.456 ***	-.003	27 ***
	GSN	.001	.409 ***	.222 *	21 ***
	GSS	.046	.448 ***	.159	26 ***
SON	Sp	.137	.735 ***	.136	<u>55 ***</u>
	Bj	.135	.715 ***	.020	39 ***
	GSN	-.269 **	.566 ***	.327 ***	43 ***
	GSS	-.060	.588 ***	.422 ***	42 ***
DJF	Sp	.047	.628 ***	.283 ***	40 ***
	Bj	.217 **	.587 ***	.175 *	<u>41 ***</u>
	GSN	-.143	.522 ***	.341 ***	30 ***
	GSS	.007	.361 ***	.243 *	17 ***

Note: R2, coefficient of determination for the multiple regression in %; *p*, statistical significance for the multiple regression; *p*, threshold of statistical significance: * ≤.05, ** ≤.01, *** ≤.001, italic underlined, highest R2; italic, lowest R2; significant cases are bolded.

TABLE 7 Statistics for multiple regression between seasonal air temperature at Björnøya station and circulation indices (Wi, Si, and Ci) for various RCAs, 1920–2018

anticyclonic and zonal circulation in spring and meridional circulation in autumn and winter, as represented by the regional indices. This section focuses on the ETCAW and aims to answer the question of whether there were any changes between the ETCAW, CAP, and CAW in the relations between SAT and regional circulation.

Particular consideration is given to whether the importance of the RCAs changed depending on the warm/cold periods. Since the ETCAW was a seasonally occurring event, we only discussed the autumn and winter and the original series (with trends). Tables 8 and 9 include the results of multiple regression between the studied

variables during the 30-year sub-periods, that is, the ETCAW, CAP, and CAW.

3.3.1 | Autumn (SON)

Considering autumn, no important temporal changes were found in the spatial pattern of regression between SAT and RCAs. In each sub-period, SAT was most strongly correlated with circulation over eastern RCAs (highest coefficients of determination R²), and of all the indexes, the Si was the most influential over each RCA. The autumn SAT at both stations was significantly related to the frequency of cyclonic conditions over the

western RCAs but the relation was insignificant in the eastern RCAs (Table 8). During the ETCAW, the impact of Si index on SAT over the eastern regions (RCA_{Sp} and RCA_{Bj}) was clearly stronger than that in the western regions (RCA_{GSN} and RCA_{GSS}). During the CAP and CAW, the regional diversity in the impact of circulation on SAT was much smaller (variation in regression coefficients for particular regions was smaller) than during the ETCAW. In the cold period (CAP), the Si, which had the lowest negative values, indicating an increased frequency of air advection from the northern sector (Table 5) over RCA_{GSN}, was stronger than in the other 30-year sub-periods (Table 8). Moreover, the frequency of air advection from the southern sector was significantly enhanced

TABLE 8 Statistical parameters of multiple regression for the composite series of SON air temperature at Svalbard Airport and Bjørnøya stations and circulation indices calculated for various regional circulation areas (RCAs) during the 30-year periods representing the ETCAW, CAP, and CAW

Regression coefficients for circulation indices						
Svalbard Airport station						
Periods		RCAs	Wi	Si	Ci	R2
1933–1962	ETCAW	RCA _{Sp}	–.126	.777 ***	.112	<u>63 ***</u>
		RCA _{Bj}	.014	.785 ***	.065	<u>63 ***</u>
		RCA _{GSN}	–.383 *	.436 **	.280	<u>42 **</u>
		RCA _{GSS}	–.218	.274	.343	22
1966–1995	CAP	RCA _{Sp}	.274 *	.728 ***	.175	<u>61 ***</u>
		RCA _{Bj}	.086	.699 ***	.016	<u>54 ***</u>
		RCA _{GSN}	–.229	.697 ***	.427 **	<u>52 ***</u>
		RCA _{GSS}	.139	.612 ***	.491 **	<u>51 ***</u>
1989–2018	CAW	RCA _{Sp}	.273 *	.664 ***	–.008	<u>63 ***</u>
		RCA _{Bj}	.168	.667 ***	–.148	<u>55 ***</u>
		RCA _{GSN}	.014	.600 ***	.370 *	<u>50 ***</u>
		RCA _{GSS}	.079	.643 ***	.301	<u>45 **</u>
Bjørnøya station						
1933–1962	ETCAW	RCA _{Sp}	–.003	.831 ***	.214	<u>67 ***</u>
		RCA _{Bj}	.097	.864 ***	.087	<u>77 ***</u>
		RCA _{GSN}	–.296	.511 **	.449 **	<u>52 ***</u>
		RCA _{GSS}	–.122	.366 *	.512 **	<u>35 **</u>
1966–1995	CAP	RCA _{Sp}	.183	.721 ***	.232	<u>57 ***</u>
		RCA _{Bj}	.108	.751 ***	.146	<u>62 ***</u>
		RCA _{GSN}	–.339 *	.663 ***	.453 **	<u>55 ***</u>
		RCA _{GSS}	.031	.572 ***	.564 ***	<u>51 ***</u>
1989–2018	CAW	RCA _{Sp}	.161	.667 ***	.176	<u>57 ***</u>
		RCA _{Bj}	.130	.696 ***	.051	<u>54 ***</u>
		RCA _{GSN}	–.121	.544 **	.515 ***	<u>51 ***</u>
		RCA _{GSS}	.004	.648 ***	.506 **	<u>52 ***</u>

Note: R², coefficient of determination for the model; p, statistical significance for the model: * ≤.05, ** ≤.01, *** ≤.001, italic underlined, highest R²; italic, lowest R²; significant cases are bolded.

		Regression coefficients for circulation indices Svalbard Airport Station				
Periods		RCA _S	Wi	Si	Ci	R2
1929–1958	ETCAW	RCA _{Sp}	.391 **	.562 ***	.003	<u>62 ***</u>
		RCA _{Bj}	.336 *	.519 ***	–.252	58 ***
		RCA _{GSN}	.110	.572 **	.104	40 **
		RCA _{GSS}	–.014	.650 **	–.080	41 **
1959–1988	CAP	RCA _{Sp}	.200	.559 **	.308	44 **
		RCA _{Bj}	.436 *	.332	–.005	40 **
		RCA _{GSN}	–.002	.646 ***	.453 *	<u>48 ***</u>
		RCA _{GSS}	.140	.461 *	.168	31 *
1989–2018	CAW	RCA _{Sp}	.358 *	.676 ***	.326 *	51 ***
		RCA _{Bj}	.391 **	.673 ***	.123	<u>53 ***</u>
		RCA _{GSN}	.189	.482 *	.259	28 *
		RCA _{GSS}	–.007	.355	.070	11
Bjørnøya station						
1929–1958	ETCAW	RCA _{Sp}	.215	.647 ***	.164	<u>54 ***</u>
		RCA _{Bj}	.292 *	.637 ***	.001	53 ***
		RCA _{GSN}	–.081	.531 **	.266	34 *
		RCA _{GSS}	–.053	.595 **	.172	36 **
1959–1988	CAP	RCA _{Sp}	.084	.694 ***	.362 *	<u>54 ***</u>
		RCA _{Bj}	.392 *	.470 **	.090	50 ***
		RCA _{GSN}	–.034	.566 **	.509 **	43 **
		RCA _{GSS}	.271	.316	.221	29 *
1989–2018	CAW	RCA _{Sp}	.249	.725 ***	.358 *	51 ***
		RCA _{Bj}	.352 *	.729 ***	.213	<u>56 ***</u>
		RCA _{GSN}	.075	.509 *	.289	25
		RCA _{GSS}	–.099	.421	.159	13

Note: R2, coefficient of determination for the model; *p*, statistical significance for the model: * ≤ .05, ** ≤ .01, *** ≤ .001, talic underlined, highest R2; italic, lowest R2; significant cases are bolded.

over all the RCAs during the ETCAW as compared to the CAW (see Table 5), which suggests that other factors might have contributed to the contemporary warming. It should also be noted that the regional circulation over eastern RCAs explained more variance in SAT during the ETCAW than during the CAW, particularly over Bjørnøya. The circulation over the western RCAs explained more variability in the SAT during the CAW than during the ETCAW, which mainly concerns Spitsbergen.

3.3.2 | Winter (DJF)

In DJF, the impact of regional atmospheric circulation on SAT was clearly smaller and more complicated than in

TABLE 9 Statistical parameters of multiple regression for the composite series of DJF air temperature at Svalbard Airport and Bjørnøya stations and circulation indices calculated for various regional circulation areas (RCAs) during the 30-year periods representing the ETCAW, CP, and CW

SON (compare Tables 9 and 8), particularly in the case of Svalbard Airport station. The only exception was the western RCAs (Greenland Sea) during the ETCAW, for which the regression between Si and SAT was stronger in winter than in autumn. The coefficient of determination for multiple regression indicated that, in particular sub-periods, various RCAs played the leading role in shaping SAT at Svalbard Airport station. Nonetheless, the impact of circulation over Spitsbergen on SAT was greater during the ETCAW than during the CAW. At Bjørnøya station, the relations were more stable. The eastern RCAs played a leading role in shaping the SAT, and the differences in the strength of the regression between the 30-year periods were small in those RCAs. In winter, similar to autumn, the Si index mostly contributed to the variability in SAT. It was also found at both stations that:

(i) the impact of Si index over RCA_{Sp} and RCA_{Bj} on SAT during CAW was higher than in the previous 30-year sub-periods (higher regression coefficients), (ii) in the CAP, the regression between SAT and Si over RCA_{Bj} was the weakest of all 30-year sub-periods, and SAT was significantly correlated with Ci over RCA_{GSN} , (iii) during the CAW, significant regression was found between SAT and Ci over RCA_{Sp} (Table 9).

4 | SUMMARY AND DISCUSSION

In this article, we discuss spatial and temporal variability in the relationship between SAT on Svalbard and regional circulation indices calculated based on the frequency of circulation types for four RCAs in the Atlantic sector of the Arctic, with a particular focus on the ETCAW. The proposed circulation indices well described the climatology of atmospheric circulation over the Atlantic sector of the Arctic and its regional differences, such as: (i) the domination of easterlies and latitudinal changes in its frequency; (ii) the domination of southern inflow in the eastern part of the study area (RCA_{Sp} and RCA_{Bj}) and the reverse situation in the western part (more frequent northerly advection); (iii) the domination of cyclonic conditions in SON and DJF, particularly in the southern part of the research area. Southern inflow over the eastern RCAs is forced by low-pressure systems that are located to the south-west of the research area (the vicinity of Iceland) or by high-pressure systems whose centres lie over the south-east of the research area (e.g., the Siberian High; Łupikasza and Niedźwiedź, 2019). The domination of northern inflow in the western part of the research area is linked to a high-pressure system developed over Greenland (Serreze and Barry, 2014). Such a constellation of sea-level pressure is reminiscent of the Barents Oscillation (BO) proposed by Chen *et al.* (2013). The highest frequency of cyclonic conditions in the southern RCAs arises from the closer location of these RCAs to the regions of cyclogenesis in the vicinity of the Icelandic Low (Serreze and Barry, 2014), which can be enhanced by the orographic effect of the southern part of the steep Greenland Ice Sheet that is termed ‘lee cyclogenesis’ (Tsukernik *et al.*, 2007), which may extend into the Barents and Kara seas (Turner and Marshall, 2011). In spring and summer, the Arctic general circulation—and cyclogenesis weakens (Zhang *et al.*, 2004; Serreze and Barry, 2014).

The existing longest chronological series of SAT for Svalbard Airport and Bjørnøya, proved that contemporary warming is the most prominent climatic event in the Arctic since the beginning of the research period (Overland *et al.*, 2012; Nordli *et al.*, 2014, 2020; Gjelt

et al., 2016). Our study showed that at both stations, the ETCAW manifested in SON and DJF. In the majority of the Arctic, warming in the first half of the 20th century was most prominent in winter and spring (Overland *et al.*, 2004), which may arise from regional variation in the warming drivers or regional modification of large-scale drivers (Shindell and Faluvegi, 2009; Yamanouchi, 2011; Johannessen *et al.*, 2016). However, modelling studies on the ETCAW indicate that autumn is the season that shows the most pronounced climate change (Holland *et al.*, 2012). In DJF, Svalbard Airport station warmed much more than Bjørnøya. The strongest warming at Svalbard Airport was confirmed by other studies (Gjelt *et al.*, 2016; Isaksen *et al.*, 2016) and was explained by decreased local sea ice cover on Isfjorden near Svalbard Airport—when the fjord is open during winter, there is an energy transfer from the fjord water to the air.

Peaks in the spring and summer SATs in the early 20th century were close to or even lower than the long-term average (1920–2018) and were also insignificantly different from the mean SAT for the subsequent CAP. Nonetheless, in these seasons, the average SAT during recent warming has been significantly higher than during the ETCAW and, in MAM, it could be partly related to changes in the Ci (more frequent cyclonic conditions during the CAW in MAM). In summer, significant changes were found in the average Wi between the ETCAW and the CAW (higher frequency of eastern advection during the CAW) over all RCAs. The increased frequency of E circulation form (according to Girs–Vangengeim typology) in the warm season over the Norwegian and Barents seas during the CAW was also indicated by Svyashchennikov *et al.* (2020). However, the regression between summer SAT at Svalbard Airport was not statistically significant for series with trends, and was negative for de-trended series. At Bjørnøya station, the regression was positive. It is possible that summer SAT at Svalbard Airport station was influenced more by the terrestrial, and thus more variable surroundings and general background warming (Isaksen *et al.*, 2016). Moreover, in summer, the most prominent centres of action weaken, and the Atlantic-Arctic becomes an area of weak low-pressure systems (Serreze and Barry, 2014; Przybylak, 2016). The impact of solar radiation is enhanced for terrestrial surfaces compared to maritime areas, which may blur, modify, or weaken the impact of atmospheric circulation.

In SON and DJF, the Si, that is, meridional air advection, had the strongest impact on SAT, particularly over the eastern regional circulation areas (RCA_{Bj} and RCA_{Sp}). However, in these seasons, most linear trends in regional circulation indices, including Si, were insignificant. Changes in SAT, particularly in SON, were

related to multi-decadal changes in regional circulation expressed by differences in average indices values between the cold and warm periods. In SON, meridional circulation contributed to warming in the early 20th century since differences in Si averages between the ETCAW and CAP were statistically significant over all RCAs. Previous studies (Overland *et al.*, 2008; Wood and Overland, 2010) also associated ETCAW with a meridional mode of atmospheric circulation that reappeared during the CAW. In addition, upper air data for the 1930s show a stronger-than-normal meridional transport of warm air into the European Arctic during the warm period compared to the preceding cold period (Grant *et al.*, 2009). Our study revealed that on a regional scale, the increase in frequency of meridional circulation was slightly lower in the CAW than during the ETCAW. Such a flow over the Nordic Seas is linked to the BO and is accompanied by zonal wind anomalies and sensible heat loss over the Barents Sea, both of which have been recognized to drive the Arctic air temperature since 1948 (Goosse and Holland, 2005; Chen *et al.*, 2013).

Modelling studies have shown that atmospheric internal variability is a significant part of the ETCAW even during winter (Wood and Overland, 2010; Beitsch *et al.*, 2014; Wegmann *et al.*, 2017). However, we found that in DJF, the increase in the frequency of the southern advection was only found over the RCA_{Sp} and Si explained much less variance in SAT (14–27% over eastern RCAs) than in SON (31–33% over eastern RCAs, not presented in the study but calculated using Pearson correlation coefficients). Hanssen–Bauer and Førland (1998) emphasized that variations in circulation pattern accounted for only a fraction of the temperature increase at the Svalbard Airport from 1912 to the 1930s and for the temperature decrease from the 1930s to the 1960s. The mixture of these various results, including the significant long-term trends in SAT, insignificant trends in Si, plus significant changes in the average values of SAT and Si over the selected RCAs, indicate the seasonal and temporal variations in the strength of the impact of various drivers of SAT change. Therefore, in winter, the ETCAW might have been more strongly influenced by a chain of processes causing heat transport to the Arctic (Suo *et al.*, 2013; Beitsch *et al.*, 2014), reduction in sea-ice, retreat of ice edge thereby resulting in enhanced ocean–atmosphere heat fluxes (Bengtsson *et al.*, 2004; Divine and Dick, 2006; Alekseev *et al.*, 2007, Alekseev *et al.*, 2009; Semenov and Latif, 2012; Beitsch *et al.*, 2014; Alekseev *et al.*, 2016; Walsh *et al.*, 2017) and Atlantic multi-decadal oscillation AMO (Johannessen *et al.*, 2016; Tokinaga *et al.*, 2017). According to Grant *et al.* (2009), a sudden increase in sulphate concentrations in an ice core from Svalbard around

1930 suggests that the aerosol might have amplified the ETCAW warming by changing the cloud long-wave emissivity. However, the modelling studies stressed that SST, sea ice, and radiative forcing are not sufficient to trigger the spatial pattern of the ETCAW (Wegmann *et al.*, 2017). Moreover, atmospheric circulation might have had an indirect impact on the ETCAW, since the oceanic inflow of warmer waters into the Barents Sea is wind-driven and is linked to the strength of westerlies forced by cyclonic atmospheric circulation (Bengtsson *et al.*, 2004; Yamanouchi, 2011). Although in our study the differences in the frequency of westerlies and cyclonic activity between the warm and cold sub-periods were not statistically significant, the western advection and the frequency of cyclonic conditions in winter were higher during the warm sub-periods than during the cold sub-periods. Generally, our study shows that in DJF, the impact of regional circulation on SAT was stronger during the ETCAW than during the CAW. This means that additional warming mechanisms may also have operated during the CAW. These mechanisms, being partly similar to those during the ETCAW, include sea-ice loss (Kauker *et al.*, 2009; Overland and Wang, 2010; Overland *et al.*, 2011, 2012; Alekseev *et al.*, 2016), increased SST (e.g., Serreze *et al.*, 2011), reduction in sulphate aerosols (Navarro *et al.*, Acosta Navarro *et al.*, 2016), increased water vapour (Park *et al.*, 2015), cloud conditions (Graversen *et al.*, 2014; Pithan and Mauritsen, 2014). During the CAW, strong anthropogenic radiative forcing (Wegmann *et al.*, 2017, Przybylak *et al.*, 2021) plays an important role. The aforementioned processes intensify the feedback mechanism and lead to the warming of all air masses, which was also confirmed recently by Isaksen *et al.* (2016). As a result of these changes, the importance of regional atmospheric circulation types in shaping SAT is diminished. Our results also show that long-term trends in atmospheric circulation fail to explain the ETCAW (no significant trend). Warming in this period was related to multi-decadal changes in the circulation indices series. This agrees with the statement that the early 20th-century warming is not a long-term variation or a short-time scale decadal variation, however, it could be defined as a multi-decadal variation (Yamanouchi, 2011).

5 | CONCLUSIONS

- The average SAT in the 30-year warm and cold sub-periods revealed significant differences between the ETCAW and the CAW in JJA and MAM. The difference between the ETCAW and the CAP was statistically significant only in SON and DJF. The ETCAW was stronger in SON than in DJF

- Circulation in the eastern RCAs has more impact on the SAT than the circulation at the western RCAs at both stations, particularly during the ETCAW
- The Si impacted the variability in SAT more than the other indices at both stations, with some exceptions in MAM and JJA. In JJA, recent warming weakened the correlations between SAT and regional atmospheric circulation at Svalbard Airport. In spring, SAT showed a stronger correlation with Wi.
- The impact of regional atmospheric circulation on the ETCAW was stronger in autumn than in winter.
- The ETCAW is more related to multi-decadal changes in regional atmospheric circulation than to long-term trends, particularly in SON.
- There is reason to attribute the ETCAW in SON to changes in regional atmospheric circulation, that is, to the increased frequency of the meridional flow (southern advection), as shown by significant differences in the mean Si index between the ETCAW and CAP.
- The relationship between SAT and circulation in the four RCAs did not show prominent differences between the warming and cooling sub-periods.
- The ETCAW was characterized by a greater regional diversity in the strength of the relationship between the SAT and the regional circulation indices (larger variation in regression coefficients for particular regions) than during the CAP and CAW.
- In the CAP, the Si index, indicating an intensified air advection from the northern sector, was more strongly correlated with SAT than in warm sub-periods.

ACKNOWLEDGEMENT

The research work was supported by the National Science Centre, Poland, grant 'Causes of the early 20th century Arctic warming' (No. 2015/19/B/ST10/02933).

The study of RP was also carried out as a part of the Research University – Initiative of Excellence: the Emerging Field "Global Environmental Changes", and "Climate Change Research Unit" at Nicolaus Copernicus University in Toruń.

ORCID

Ewa B. Łupikasza  <https://orcid.org/0000-0002-3910-9076>

Rajmund Przybylak  <https://orcid.org/0000-0003-4101-6116>

REFERENCES

Acosta Navarro, J.C., Varma, V., Riipinen, I., Seland, Ø., Kirkevåg, A., Struthers, H., Iversen, T., Hansson, H.-C., and Ekman A.M.L. (2016) Amplification of Arctic warming by past

air pollution reductions in Europe. *Nature Geoscience*, 9, 277–281. <https://doi.org/10.1038/ngeo2673>.

Alekseev, G., Glok, N. and Smirnov, A. (2016) On assessment of the relationship between changes of sea ice extent and climate in the Arctic. *International Journal of Climatology*, 36(9), 3407–3412. <https://doi.org/10.1002/joc.4550>.

Alekseev, G.V., Danilov, A.I., Kattsov, V.M., Kuzmina, S.I. and Ivanov, N.E. (2009) Changes in the climate and sea ice of the Northern Hemisphere in the 20th and 21st centuries from data of observations and modelling. *Izvestiya, Atmospheric and Oceanic Physics*, 45, 675–686. <https://doi.org/10.1134/s0001433809060012>.

Alekseev, G.V., Kuzmina, S.I., Nagurny, A.P., and Ivanov, N.E. (2007) Arctic sea ice data sets in the context of the climate change during the 20th century. In: *Climate Variability and Extremes During the Past 100 Years*. Advances in Global Change Research, Springer, pp. 47–63.

Bastien, P., Esposito Vinzi, V. and Tenenhaus, M. (2005) PLS generalised regression. *Computational Statistics and Data Analysis*, 48, 17–46.

Beitsch, A., Jungclaus, J.H. and Zanchettin, D. (2014) Patterns of decadal-scale Arctic warming events in simulated climate. *Climate Dynamics*, 43, 1773–1789.

Bengtsson, L., Semenov, V.A. and Johannessen, O.M. (2004) The early twentieth-century warming in the Arctic – a possible mechanism. *Journal of Climate*, 17(20), 4045–4057. [https://doi.org/10.1175/1520-0442\(2004\)017<4045:TETWIT>2.0.CO;2](https://doi.org/10.1175/1520-0442(2004)017<4045:TETWIT>2.0.CO;2).

Bezeau, P., Sharp, M. and Gascon, G. (2015) Variability in summer anticyclonic circulation over the Canadian Arctic Archipelago and west Greenland in the late 20th/early 21st centuries and its effect on glacier mass balance. *International Journal of Climatology*, 35(4), 540–557. <https://doi.org/10.1002/joc.4000>.

Brennan, M.K., Hakim, G.J. and Blanchard-Wrigglesworth, E. (2020) Arctic sea-ice variability during the instrumental era. *Geophysical Research Letters*, 47(7), e2019GL086843. <https://doi.org/10.1029/2019GL086843>.

Brönnimann, S. (2015) *Climate Changes Since 1700*. Advances in Global Change Research. Vol. 25. Cham: Springer, 360 pp.

Cantrell, C.A. (2008) Technical Note: review of methods for linear least-squares fitting of data and application to atmospheric chemistry problems. *Atmospheric Chemistry and Physics*, 8, 5477–5487.

Champagne, O., Pohl, B., McKenzie, S., Buoncristiani, J.-F., Bernard, E., Joly, D. and Tolle, F. (2019) Atmospheric circulation modulates the spatial variability of temperature in the Atlantic–Arctic region. *International Journal of Climatology*, 39(8), 3619–3638. <https://doi.org/10.1002/joc.6044>.

Chen, H.W., Zhang, Q., Körnich, H. and Chen, D. (2013) A robust mode of climate variability in the Arctic: the Barents Oscillation. *Geophysical Research Letters*, 40, 2856–2861. <https://doi.org/10.1002/grl.50551>.

Compo, G.P., Whitaker, J.S., Sardeshmukh, P.D., Matsui, N., Allan, R.J., Yin, X., Gleason, B.E., Vose, R.S., Rutledge, G., Bessemoulin, P., Brönnimann, S., Brunet, M., Crouthamel R.I., Grant A.N., Groisman P.Y., Jones P.D., Kruk M.C., Kruger A. C., Marshall G.J., Maugeri M., Mok H.Y., Nordli Ø., Ross T.F., Trigo, R.M., Wang, X.L., Woodruff, S.D., and Worley, S.J. (2011) The Twentieth Century Reanalysis Project. *Quarterly*

- Journal Royal Meteorological Society*, 137, 1–28. <https://doi.org/10.1002/qj.776>.
- Delworth, T.L. and Knutson, T.R. (2000) Simulation of early 20th century global warming. *Science*, 287, 2246–2250.
- Ding, Q., Schweiger, A., L'Heureux, M., Battisti, D.S., Po-Chedley, S., Johnson, N.C., Blanchard-Wrigglesworth, E., Harnos, K., Zhang, Q., Eastman, R. and Steig, E.J. (2017) Influence of high-latitude atmospheric circulation changes on summertime Arctic sea ice. *Nature Climate Change*, 7, 289–295. <https://doi.org/10.1038/nclimate3241>.
- Divine, D.V. and Dick, C. (2006) Historical variability of sea ice edge position in the Nordic Seas. *Journal of Geophysical Research: Oceans*, 111, C01001. <https://doi.org/10.1029/2004jc002851>.
- Fettweis, X., Tedesco, M., van den Broeke, M. and Ettema, J. (2011) Melting trends over the Greenland ice sheet (1958–2009) from spaceborne microwave data and regional climate models. *The Cryosphere*, 5(2), 359–375. <https://doi.org/10.5194/tc-5-359-2011>.
- Gjelten, H.M., Nordli, Ø., Isaksen, K., Førland, E.J., Sviashchennikov, P.N., Wyszynski, P., Prokhorova, U.V., Przybylak, R., Ivanov, B.V. and Urazgildeeva, A.V. (2016) Air temperature variations and gradients along the coast and fjords of western Spitsbergen. *Polar Research*, 35, 29878. <https://doi.org/10.3402/polar.v35.29878>.
- Goosse, H. and Holland, M.M. (2005) Mechanisms of decadal Arctic climate variability in the Community Climate System Model, Version 2 (CCSM2). *Journal of Climate*, 18(17), 3552–3570. <https://doi.org/10.1175/JCLI3476.1>.
- Grant, A.N., Brönnimann, S., Ewen, T., Griesser, T. and Strickler, A. (2009) The early twentieth century warm period in the European Arctic. *Meteorologische Zeitschrift*, 18(4), 425–432. <https://doi.org/10.1127/0941-2948/2009/0391>.
- Graversen, R.G., Langen, P.L. and Mauritsen, T. (2014) Polar amplification in CCSM4: contributions from the lapse rate and surface albedo feedbacks. *Journal of Climate*, 27(12), 4433–4450. <https://doi.org/10.1175/JCLI-D-13-00551.1>.
- Groissmayer, F.B. (1943) Die Grosse Säkuläre Klimawende seit 1940. *Annalen der Hydrographie und Maritimen Meteorologie*, März 1943, S.79.
- Hanna, E., Fettweis, X. and Hall, R.J. (2018) Brief communication: recent changes in summer Greenland blocking captured by none of the CMIP5 models. *The Cryosphere*, 12(3287–3292), 2018–3292. <https://doi.org/10.5194/tc-12-3287-2018>.
- Hanna, E., Jones, J.M., Cappelen, J., Mernild, S.H., Wood, L., Steffen, K. and Huybrechts, P. (2013) The influence of North Atlantic atmospheric and oceanic forcing effects on 1900–2010 Greenland summer climate and ice melt/runoff. *International Journal of Climatology*, 33, 862–880.
- Hanssen-Bauer, I. and Førland, E.J. (1998) Long-term trends in precipitation and temperature in the Norwegian Arctic: can they be explained by changes in atmospheric circulation patterns? *Climate Research*, 10(2), 143–153.
- Hegerl, G.C., Brönnimann, S., Schurer, A. and Cowan, T. (2018) The early 20th century warming: anomalies, causes, and consequences. *Wiley WIREs Climate Change*, 9(4), e522. <https://doi.org/10.1002/wcc.522>.
- Hesselberg, T.H. and Birkeland, B.J. (1940) Säkuläre Schwankungen des Klimas von Norwegen, Teil I: Die Lufttemperatur. *Geophysics*, 14, 4.
- Holland, M.M., Bailey, D.A., Briegleb, B.P., Light, B. and Hunke, E. (2012) Improved sea ice shortwave radiation physics in CCSM4: the impact of melt ponds and aerosols on Arctic sea ice. *Journal of Climate*, 25(5), 1413–1430.
- Huang, X.-T., Diao, Y.-N. and Luo, D.-H. (2017) Amplified winter Arctic tropospheric warming and its link to atmospheric circulation changes. *Atmospheric and Oceanic Science Letters*, 10(6), 435–445. <https://doi.org/10.1080/16742834.2017.1394159>.
- Isaksen, K., Nordli, Ø., Førland, E.J., Łupikasza, E., Eastwood, S. and Niedźwiedź, T. (2016) Recent warming on Spitsbergen— influence of atmospheric circulation and sea ice cover. *Journal of Geophysical Research: Atmospheres*, 121(20), 11913–11931. <https://doi.org/10.1002/2016JD025606>.
- Johannessen, O.M., Bengtsson, L., Miles, M.W., Kuzmina, S.I., Semenov, V.A., Alekseev, G.V., Nagurnyi, A.P., Zakharov, V.F., Bobylev, L.P., Pettersson, L.H., Hasselmann, K. and Cattle, A.P. (2004) Arctic climate change: observed and modelled temperature and sea-ice variability. *Tellus Series A: Dynamic Meteorology and Oceanography*, 56A(4), 328–341.
- Johannessen, O.M., Kuzmina, S.I., Bobylev, L.P. and Miles, M.W. (2016) Surface air temperature variability and trends in the Arctic: new amplification assessment and regionalisation. *Tellus Series A: Dynamic Meteorology and Oceanography*, 68A, 28234. <https://doi.org/10.3402/tellusa.v68.28234>.
- Kalnay, E., Kanamitsu, M., Kistler, R., Collins, W., Deaven, D., Gandin, L., Iredell, M., Saha, S., White, G., Woollen, J., Zhu, Y., Chelliah, M., Ebisuzaki, W., Higgins, W., Janowiak, J., Mo, K. C., Ropelewski, C., Wang, J., Leetmaa, A., Reynolds, R., Jenne, R., and Joseph, D., (1996) The NCEP/NCAR 40-year Reanalysis Project. *Bulletin of the American Meteorological Society*, 77, 437–471.
- Kauker, F., Kaminski, T., Karcher, M., Giering, R., Gerdes, R. and Voßbeck, M. (2009) Adjoint analysis of the 2007 all time Arctic sea-ice minimum. *Geophysical Research Letters*, 36(3), L03707. <https://doi.org/10.1029/2008GL036323>.
- Kelly, P.M., Jones, P.D., Sear, C.B., Cherry, B.S.G. and Tavakol, R. K. (1982) Variation in surface air temperatures: Part 2. Arctic Regions, 1881–1980. *Monthly Weather Review*, 110, 71–83.
- Knipovich, I.M. (1921) Thermic conditions in the Barents Sea at the end of May, 1921. *Byulletin Rossiiskogo Gidrologiceskogo Instituta*, 9, 10–12 (in Russian).
- Lamb, H.H. and Johnsson, A.I. (1959) Climatic variation and observed changes in the general circulation. Parts I and II. *Geografiska Annaler (Stockholm)*, 41, 94–134.
- Łupikasza, E.B. and Niedźwiedź, T. (2019) The influence of meso-scale atmospheric circulation on Spitsbergen air temperature in periods of Arctic warming and cooling. *Journal of Geophysical Research: Atmospheres*, 124(10), 5233–5250. <https://doi.org/10.1029/2018JD029443>.
- Lysgaard, L. (1949) Recent climatic fluctuations. *Folia Geographica Danica*, V, København, 86 pp.
- Miles, M.W., Divine, D.V., Furevik, T., Jansen, E., Moros, M. and Ogilvie, A.E.J. (2014) A signal of persistent Atlantic multi decadal variability in Arctic sea ice. *Geophysical Research Letters*, 41, 463–469. <https://doi.org/10.1002/2013GL058084>.
- Murray, R. and Lewis, R.P. (1966) Some aspects of the synoptic climatology of the British Isles as measured by simple indices. *Meteorological Magazine*, 95, 193–203.

- Niedźwiedz, T. (1993) The main factors forming the climate of the Hornsund (Spitsbergen). *Zeszyty Naukowe UJ, Prace Geograficzne. Kraków*, 94, 49–63.
- Niedźwiedz, T. (2013) Changes of circulation indices. Chapter 16.2. In: Marsz, A.A. and Styszyńska, A. (Eds.) *Climate and Climate Change at Hornsund, Svalbard*. Gdynia: Gdynia Maritime University, pp. 285–292.
- Nordli, Ø., Przybylak, R., Ogilvie, A.E.J. and Isaksen, K. (2014) Long-term temperature trends and variability on Spitsbergen: the extended Svalbard Airport temperature series, 1898–2012. *Polar Research*, 33(1), 21349. <https://doi.org/10.3402/polar.v33.21349>.
- Nordli, Ø., Wyszyński, P., Gjeltén, H.M., Isaksen, K., Łupikasza, E., Niedźwiedz, T. and Przybylak, R. (2020) Revisiting the extended Svalbard Airport monthly temperature series, and the compilation of a corresponding daily series 1898–2018. *Polar Research*, 39, 3614. <https://doi.org/10.33265/polar.v39.3614>.
- Nozawa, T., Nagashima, T., Shiogama, H. and Crooks, S.A. (2005) Detecting natural influence on surface air temperature change in the early twentieth century. *Geophysical Research Letters*, 32(20), L20719. <https://doi.org/10.1029/2005GL023540>.
- Ogi, M., Søren, R. and Barber, D.G. (2016) The influence of winter and summer atmospheric circulation on the variability of temperature and sea ice around Greenland. *Tellus A: Dynamic Meteorology and Oceanography*, 68(1), 31971. <https://doi.org/10.3402/tellusa.v68.31971>.
- Overland, J.E., Francis, J.A., Hanna, E. and Wang, M. (2012) The recent shift in early summer Arctic atmospheric circulation. *Geophysical Research Letters*, 39(19), L19804. <https://doi.org/10.1029/2012GL053268>.
- Overland, J.E., Spillane, M.C., Percival, D.B., Wang, M. and Mofjeld, H.O. (2004) Seasonal and regional variation of Pan-Arctic surface air temperature over the instrumental record. *Journal of Climate*, 17(17), 3263–3282. [https://doi.org/10.1175/1520-0442\(2004\)017<3263:SARVOP>2.0.CO;2](https://doi.org/10.1175/1520-0442(2004)017<3263:SARVOP>2.0.CO;2).
- Overland, J.E. and Wang, M. (2010) Large-scale atmospheric circulation changes are associated with the recent loss of Arctic sea ice. *Tellus Series A: Dynamic Meteorology and Oceanography*, 62A(1), 1–9. <https://doi.org/10.1111/j.1600-0870.2009.00421.x>.
- Overland, J.E., Wang, M. and Salo, S. (2008) The recent Arctic warm period. *Tellus Series A: Dynamic Meteorology and Oceanography*, 60A(4), 589–597. <https://doi.org/10.1111/j.1600-0870.2008.00327.x>.
- Overland, J.E., Wood, K. and Wang, M. (2011) Warm Arctic - cold continents: climate impacts of the newly open Arctic Sea. *Polar Research*, 30, 15787. <https://doi.org/10.3402/polar.v30i0.15787>.
- Park, D.-S.R., Lee, S. and Feldstein, S.B. (2015) Attribution of the recent winter sea ice decline over the Atlantic sector of the Arctic Ocean. *Journal of Climate*, 28(10), 4027–4033. <https://doi.org/10.1175/JCLI-D-15-0042.1>.
- Petterssen, S. (1949) Changes in the general circulation associated with the recent climatic variations. *Geografiska Annaler (Stockholm)*, 31(1–2), 212–221.
- Piechura, J. and Walczowski, W. (2009) Warming of the West Spitsbergen Current and sea ice north of Svalbard. *Oceanologia*, 51(2), 147–164 <http://www.iopan.gda.pl/oceanologia/>.
- Pithan, F. and Mauritsen, T. (2014) Arctic amplification dominated by temperature feedbacks in contemporary climate models. *Nature Geoscience*, 7(3), 181–184.
- Polyakov, I.V., Timokhov, L.A., Alexeev, V.A., Bacon, S., Dmitrenko, I.A., Fortier, L., Frolov, I.E., Gascard, J.-C., Hansen, E., Ivanov, V.V., Laxon, S., Mauritsen, C., Perovich, D., Shimada, K., Simmons, H.L., Sokolov, V.T., Steele, M. and Toole, J. (2010) Arctic Ocean warming contributes to reduced polar ice cap. *Journal of Physical Oceanography*, 40(12), 2743–2756.
- Przybylak, R. (2000) Temporal and spatial variation of air temperature over the period of instrumental observations in the Arctic. *International Journal of Climatology*, 20(6), 587–614. [https://doi.org/10.1002/\(SICI\)1097-0088\(200005\)20:6<587::AID-JOC480>3.0.CO;2-H](https://doi.org/10.1002/(SICI)1097-0088(200005)20:6<587::AID-JOC480>3.0.CO;2-H).
- Przybylak, R. (2002) *Variability of Air Temperature and Atmospheric Precipitation in the Arctic*. Atmospheric and Oceanographic Sciences Library, Vol. 25. Dordrecht/Boston/London: Kluwer Academic Publishers, p. 330.
- Przybylak, R. (2016) *The Climate of the Arctic*, 2nd edition. Cham, Switzerland: Springer. 287 pp. <https://doi.org/10.1007/978-3-319-21696-6>.
- Przybylak, R., Svyashchennikov, P.N., Uscka-Kowalkowska, J. and Wyszyński, P. (2021) Solar radiation in the Arctic during the Early Twentieth Century Warming (1921–1950), presenting a compilation of newly available data. *Journal of Climate*, 34(1), 21–37. <https://doi.org/10.1175/JCLI-D-20-0257.1>.
- Robock, A. (2000) Volcanic eruptions and climate. *Reviews of Geophysics*, 38(2), 191–219. <https://doi.org/10.1029/1998RG000054>.
- Scherhag, R. (1931) Eine bemerkungswerte Klimaänderung über Nord-Europa. *Annalen der Hydrographie und Maritimen Meteorologie*, 57–67.
- Scherhag, R. (1937) Die Erwärmung der Arktis. *ICES Journal of Marine Science*, 12(3), 263–276. <https://doi.org/10.1093/icesjms/12.3.263>.
- Scherhag, R. (1939) *Die Erwärmung des Polargebiets. Annalen der Hydrographie und Maritime Meteorologie*, 67, 57–67.
- Semenov, V.A. (2007) Structure of temperature variability in the high latitudes of the Northern Hemisphere. *Izvestiya - Atmospheric and Ocean Physics*, 43(6), 687–695. <https://doi.org/10.1134/S0001433807060023>.
- Semenov, V.A. and Latif, M. (2012) The early twentieth century warming and winter Arctic sea ice. *The Cryosphere*, 6(6), 1231–1237. <https://doi.org/10.5194/tc-6-1231-2012>.
- Serreze, M.C., Barrett, A.P. and Cassano, J.J. (2011) Circulation and surface controls on the lower tropospheric air temperature field of the Arctic. *Journal of Geophysical Research*, 116, D07104. <https://doi.org/10.1029/2010JD015127>.
- Serreze, M.C. and Barry, R.G. (1988) Synoptic activity in the Arctic Basin, 1979–85. *Journal of Climate*, 1(12), 1276–1295. [https://doi.org/10.1175/1520-0442\(1988\)001<1276:SAITAB>2.0.CO;2](https://doi.org/10.1175/1520-0442(1988)001<1276:SAITAB>2.0.CO;2).
- Serreze, M.C. and Barry, R.G. (2014) *The Arctic Climate System*, 2nd edition. Cambridge: Cambridge University Press, p. 404.
- Serreze, M.C., Carse, F. and Barry, R.G. (1997) Icelandic low cyclone activity: climatological features, linkages with the NAO, and relationships with recent changes in the northern hemisphere circulation. *Journal of Climate*, 10, 453–464.
- Serreze, M.C. and Francis, J.A. (2006) The Arctic amplification debate. *Climatic Change*, 76(3–4), 241–264.
- Serreze, M.C., Walsh, J.E., Chapin, F.S.I.I.I., Osterkamp, T., Dyurgerov, M., Romanovsky, V., Oechel, W.C., Morison, J.,

- Zhang, T. and Barry, R.G. (2000) Observational evidence of recent change in the northern high-latitude environment. *Climatic Change*, 46, 159–207.
- Shindell, D. and Faluvegi, G. (2009) Climate response to regional radiative forcing during the twentieth century. *Nature Geoscience*, 2, 294–300. <https://doi.org/10.1038/NGEO473>.
- Shiogama, H., Nagashima, T., Yokohata, T., Crooks, S.A. and Nozawa, T. (2006) Influence of volcanic activity and changes in solar irradiance on surface air temperatures in the early twentieth century. *Geophysical Research Letters*, 33, L09702. <https://doi.org/10.1029/2005GL025622>.
- Suo, L., Otterå, O.H., Bentsen, M., Gao, Y. and Johannessen, O.M. (2013) External forcing of the early 20th century Arctic warming. *Tellus A: Dynamic Meteorology and Oceanography*, 65(1), 20578. <https://doi.org/10.3402/tellusa.v65i0.20578>.
- Svyashchennikov, P.N., Prokhorova, U.V. and Ivanov, B.V. (2020) Comparison of atmospheric circulation in the area of Spitsbergen in 1920–1950 and in the modern warming period. *Russian Meteorology and Hydrology*, 45(1), 22–28.
- Tokinaga, H., Xie, S.P. and Mukougawa, H. (2017) Early 20th-century Arctic warming intensified by Pacific and Atlantic multidecadal variability. *PNAS*, 114(24), 6227–6232. <https://doi.org/10.1073/pnas.1615880114>.
- Tsukernik, M., Kindig, D.N. and Serreze, M.C. (2007) Characteristics of winter cyclone activity in the northern North Atlantic: insights from observations and regional modelling. *Journal of Geophysical Research*, 112, D03101. <https://doi.org/10.1029/2006JD007184>.
- Turner, J. and Marshall, G.J. (2011) *Climate Change in the Polar Regions*. Cambridge: Cambridge University Press, p. 448.
- Vize, V.Y. (1940) *The Sea Climate in the Russian Arctic*. Moscow: Izd-vo Glavsevmorputi, Leningrad 124 pp. (in Russian).
- Walsh, J.E., Fetterer, F., Steward, J.S. and Chapman, W.L. (2017) A database for depicting Arctic sea ice variations back to 1850. *Geographical Review*, 107(1), 89–107.
- Wang, Y., Bi, H., Huang, H., Liu, Y., Liu, Y., Liang, X., Fu, M. and Zhang, Z. (2019) Satellite-observed trends in the Arctic sea ice concentration for the period 1979–2016. *Journal of Oceanology and Limnology*, 37, 18–37. <https://doi.org/10.1007/s00343-019-7284-0>.
- Wegmann, M., Brönnimann, S. and Compo, G.P. (2017) Tropospheric circulation during the early twentieth century Arctic warming. *Climate Dynamics*, 48(7–8), 2405–2418. <https://doi.org/10.1007/s00382-016-3212-6>.
- Wegmann, M., Orsolini, Y. and Zolina, O. (2018) Warm Arctic - cold Siberia: comparing the recent and the early 20th-century Arctic warmings. *Environmental Research Letters*, 13(2), 025009. <https://doi.org/10.1088/1748-9326/aaa0b7>.
- Weickmann, L. (1942) Zur Diskussion der Arktis zugeführten Wärmemenge. Die Erwärmung der Arktis. Veröff. Deutschen Wiss. Inst. Kopenhagen.
- Wilks, D.S. (2019) *Statistical Methods in the Atmospheric Sciences*, 4th edition. Netherlands: Elsevier Science 840 pp.
- Wold, S. (1995) PLS for multivariate linear modelling. In: van de Waterbeemd, H. (Ed.) *QSAR: Chemometric Methods in Molecular Design*, Vol. 2. Germany: Wiley-VCH, Weinheim, pp. 195–218.
- Wood, K.R. and Overland, J.E. (2010) Early 20th century Arctic warming in retrospect. *International Journal of Climatology*, 30(9), 1269–1279. <https://doi.org/10.1002/joc.1973>.
- Yamanouchi, T. (2011) Early 20th century warming in the Arctic: a review. *Polar Science*, 5(1), 53–71. <https://doi.org/10.1016/j.polar.2010.10.002>.
- Zhang, X.D., Walsh, J.E., Zhang, J., Bhatt, U.S. and Ikeda, M. (2004) Climatology and interannual variability of Arctic cyclone activity: 1948–2002. *Journal of Climate*, 17(12), 2300–2317. [https://doi.org/10.1175/1520-0442\(2004\)017<2300:CAIVOA>2.0.CO;2](https://doi.org/10.1175/1520-0442(2004)017<2300:CAIVOA>2.0.CO;2).

How to cite this article: Łupikasza EB, Niedźwiedz T, Przybylak R, Nordli Ø. Importance of regional indices of atmospheric circulation for periods of warming and cooling in Svalbard during 1920–2018. *Int J Climatol*. 2021;41:3481–3502. <https://doi.org/10.1002/joc.7031>